SUSTAINABLE STRATEGIES FOR ELECTRIC VEHICLE WASTE MANAGEMENT: A STUDY ON FORECASTING AND SITE SUITABILITY ANALYSIS

M.Tech. Thesis

By

RAHUL KUMAR YADAV

(2302104016)

DEPARTMENT OF CIVIL ENGINEERING

INDIAN INSTITUTE OF TECHNOLOGY INDORE

MAY 2025

SUSTAINABLE STRATEGIES FOR ELECTRIC VEHICLE WASTE MANAGEMENT: A STUDY ON FORECASTING AND SITE SUITABILITY ANALYSIS

A THESIS

Submitted in partial fulfilment of the
requirements for the award of the degree
of
Master of Technology

by

RAHUL KUMAR YADAV
(2302104016)

DEPARTMENT OF CIVIL ENGINEERING

INDIAN INSTITUTE OF TECHNOLOGY INDORE

MAY 2025

INDIAN INSTITUTE OF TECHNOLOGY INDORE

CANDIDATE'S DECLARATION

I hereby certify that the work which is being presented in the thesis entitled **SUSTAINABLE STRATEGIES FOR ELECTRIC VEHICLE WASTE MANAGEMENT: A STUDY ON FORECASTING AND SITE SUITABILITY ANALYSIS** in the partial fulfillment of the requirements for the award of the degree of **MASTER OF TECHNOLOGY** and submitted in the **DEPARTMENT OF CIVIL ENGINEERING, Indian Institute of Technology Indore**, is an authentic record of my own work carried out during the time period from **July 2023** to **May 2025** under the supervision of **Dr. Ashootosh Mandpe,** Assistant Professor, Department of Civil Engineering.

The matter presented in this thesis has not been submitted by me for the award of any other degree of this or any other institute.

Rahul Kum. Yadav
23-05-2025

Signature of the student with date
RAHUL KUMAR YADAV

This is to certify that the above statement made by the candidate is correct to the best of my knowledge.

Mandpe.

(23-05-2025)
Signature of the Supervisor of
M.Tech. thesis #1 (23-05-2025)
(Dr. Ashootosh Mandpe)

RAHUL KUMAR YADAV has successfully given his M.Tech. Oral Examination held on **May 24, 2025**.

Mandpe.

Signature(s) of Supervisor(s) of M.Tech. thesis
Date: 30-05-2025

Convener, DPGC
Date: 30-05-2025

ACKNOWLEDGEMENTS

I would like to express my deepest gratitude to my supervisor, **Dr. Ashootosh Mandpe**, **Assistant Professor, Department of Civil Engineering**, for his invaluable guidance, constant encouragement, and insightful feedback throughout my research journey. His expertise, patience, and unwavering support have been instrumental in shaping this thesis. His constructive criticism and motivation have not only helped me grow as a researcher but also inspired me to strive for excellence.

I extend my heartfelt thanks to **Dr. Abhishek Rajput**, **Head of the Department, Department of Civil Engineering,** for his support and encouragement, which provided a conducive academic environment for my research. I am also thankful to **Prof. Suhas S. Joshi, Director of IIT Indore**, for facilitating a research-oriented atmosphere and providing the necessary infrastructure and resources throughout my study.

I am also grateful to my lab-mates, seniors, and batchmates, especially from water climate and sustainability specialisation, for their continuous support, stimulating discussions, and camaraderie. Their assistance—whether in brainstorming ideas, troubleshooting technical challenges, or simply offering moral support—made this journey smoother and more enjoyable. A special thanks to my parents, family members for their support, encouragement, and help during this low phase of my academic life. Their belief in me kept me motivated even during the most challenging times.

Lastly, I acknowledge all the researchers and authors whose work has contributed to the foundation of this study. Their contributions have been crucial in shaping my research.

This accomplishment would not have been possible without the collective support of everyone mentioned above, and I sincerely appreciate their role in my academic journey.

Abstract

The rapid adoption of Electric Vehicles (EVs) in India, particularly electric two-wheelers (E2Ws), has amplified the urgency for sustainable end-of-life (EOL) EV lithium-ion battery (LIB) management. This thesis presents an integrated approach to forecasting LIB waste generation from E2Ws and identifying suitable locations for establishing a LIB recycling facility in Indore, India. A Seasonal Autoregressive Integrated Moving Average (SARIMA) model was developed using 94 months of historical E2Ws sales data (2017–2024) sourced from the VAHAN portal. The model demonstrated robust forecasting accuracy with an R^2 value of 0.70 and an MAPE of 10.8%, effectively capturing both seasonal and non-seasonal patterns in EV adoption. Forecasts extended through 2030 were used to project future battery waste, considering average battery capacities and a base-case specific energy of 210 Wh/kg. Battery EOL contributions were assessed across three lifespan scenarios (4, 6, and 8 years), providing scenario-based waste timelines that align with practical battery degradation behaviour.

In parallel, a GIS-based site suitability analysis was conducted using the Analytical Hierarchy Process (AHP) combined with spatial datasets including land use, proximity to roads, water bodies, industrial zones, slope, and elevation. The results identify optimal locations in the Indore district for LIB recycling infrastructure development, ensuring environmental compliance, logistical feasibility, and urban integration.

This research delivers a novel methodological framework tailored to Indian conditions for linking EV market growth with battery waste forecasting and strategic infrastructure planning. The outcomes support policymakers, industry stakeholders, and urban planners in anticipating LIB waste flows, optimising recycling operations, and accelerating India's transition towards a circular economy in the EV sector.

The integration of spatial and temporal analysis offers a practical tool for policymakers and planners to align infrastructure development with projected battery waste volumes. This study not only quantifies future waste but also provides actionable insights into regional infrastructure planning, supporting India's sustainable EV transition.

TABLE OF CONTENTS

LIST OF FIGURES

LIST OF TABLES

Chapter 1

Introduction

1 Introduction

Lithium-ion batteries (LIBs) have revolutionised the energy storage sector, making them an essential component of modern technologies such as Electric Vehicles (EVs), consumer electronics, and renewable energy systems. This acceptance has been made possible by the increasing energy density, longer service life, and lower self-discharge rates of such secondary batteries when compared to the traditional ones (Xu et al., 2021). Given current global efforts to switch to sustainable energy sources, LIBs are expected to boom in demand in the coming years. The report by the International Energy Agency (IEA) states that demand for EVs will increase ten times in about eight years by 2030, exacerbating the use and waste of lithium batteries (International Energy Agency (IEA), 2022).

Even though LIBs encourage the use of clean energy, which in turn helps to mitigate climate change effects through the reduction of greenhouse gases, they become a threat to the environment at the end of their useful life. Improper disposal carries the risk of leaching dangerous chemicals into the surroundings, such as lithium, cobalt, and nickel, that poison land, water, and biosystems (Ai et al., 2019). There is, therefore, a need to devise waste management techniques that can contain such environmental hazards while enabling the recovery of precious materials from waste.

The increase in demand for LIBs presents another significant challenge: the appropriate disposal and recycling of spent batteries. In this regard, a study by X. Zhang et al., (2020) has indicated that the volume of LIB waste produced is anticipated to surpass 2 billion metric tonnes yearly around 2030 in the foreseeable future. This increase in the amount of battery waste calls for accurate estimated future waste generation models. This is because forecasting is fundamental in enabling various activities, including the planning of recycling plants by governments and industries, the formulation of circular economy policies and strategies, as well as sustainable battery usage policies.

The study has these aims in mind and focuses on three key aspects of LIB waste management: forecasting the amount of waste to be produced, devising solutions for recycling applicable at the local level, and finally, analysing the impact of batteries on the environment. Such initiatives are essential in alleviating the negative effects of global warming and emerging

sustainable development issues. The drivers' quick shift towards EVs may occur with lower emissions of greenhouse gases yet poses a two-edged problem in that there is the quest for more lithium, cobalt, nickel, and other finite mineral resources, alongside environmental concerns due to poor management of LIBs at the end of their life. In providing the models to predict waste and the site-specific strategies for waste recycling, this research aids in reducing waste generation and the unnecessary exploitation of natural resources.

Such a framework is intended to facilitate the financing of the sustainable and circular economy for EV batteries, which respond to some of the key United Nations Sustainable Development Goals (SDGs), namely Responsible Consumption and Production (SDG 12) and Climate Action (SDG 13). It underscores the importance of eco-friendly approaches that seek an equilibrium between economic growth and environmental protection. This study seeks to make recommendations that will help decision-makers, city managers, and business owners alleviate the effects of LIB waste on the climate, deal with challenges to sustainable development, and strengthen the ability of the EV ecosystem to cope with changes in the environment.

Most conventional approaches for waste management focus on the use of the straight-line model or the extrapolation of past data and incorporate seasonal variations and irregular factors. Regarding the generation of waste from LIBs, various temporal influences such as % society-switching-to-EV-over-time, technological improvement and battery life span lead to variation in its temporal structure. Hence, sophisticated forecasting techniques are necessary to tackle these problems and make accurate predictions.

The global shift toward electric mobility has ushered in a new era of energy storage demands, particularly in the form of LIBs. As EVs become increasingly prevalent, so too does the volume of EOL LIBs require safe and sustainable disposal or recycling. This concern is especially pertinent in the Indian context, where the market for E2Ws and four-wheelers is expanding rapidly due to government incentives, technological advances, and environmental concerns.

In India alone, the EV market is projected to reach 10 million annual sales by 2030, with two-wheelers comprising approximately 70% of the demand, according to a recent report by (Electric Vehicles: Electric Vehicle Industry in India and Its Growth, 2025) India's EV stock exceeded 3 million units by the end of 2022 and is expected to grow exponentially. As the first generation of LIB-powered EVs approaches the end of its operational life, the country faces a looming wave of battery waste. By 2030. LIBs contain valuable but hazardous materials such as lithium, cobalt, and nickel(Dobó et al., 2023). Improper disposal can lead to environmental

degradation and safety hazards (Boyden et al., 2016). while efficient recycling can support resource recovery and circular economy goals. Given the scale of anticipated battery waste, it is imperative to develop infrastructure for environmentally sound and economically viable recycling. However, selecting an optimal site for a LIB recycling plant involves complex considerations, including proximity to battery waste generation centres, environmental sensitivity, land use compatibility, and infrastructural accessibility.

This thesis aims to perform a site suitability analysis for establishing a LIB recycling plant, with a focus on spatial distribution and future forecasting of battery waste generated from EVs and other consumer electronics. A multi-criteria decision-making (MCDM) approach integrated with Geographic Information Systems (GIS) will be employed to evaluate spatial variables such as Land Use Land Cover, road networks, Industrial Area, slope, and proximity to surface water bodies. The analysis is supported by forecasting models to predict the quantity and geographical origin of battery waste from EVs up to 2035. By integrating spatial analysis with battery waste forecasting, this research contributes to both academic knowledge and practical planning for sustainable e-waste management in India.

Chapter 2

Literature Review

2. Literature review

Recycling Technologies: The recycling of LIBs employs various techniques that could be termed hydrometallurgical or pyrometallurgical. Liu et al., (2022) In their systematic review, they stated that these techniques abandon the use of environmentally hazardous processes. The authors delve into processes like selective leaching, which have been developed to optimise the recovery of the metals present in spent batteries.

Economic and Environmental Benefits of Recycling: The cost-effectiveness of LIBs and other battery recycling systems has been supported by the analysis by Ahmad et al. (2021). The study researched the cost and pollution benefits that come with the production process, where lithium, cobalt, nickel, and more metals are used in battery manufacture. The study also established that recycling materials could cut down GHG emissions by approximately 60% when compared to normal mining processes.

The Perspective of Circular Economy Consideration: Chenet al., (2023) suggest a circular economy for LIB management while arguing that spent batteries and their components should be recycled and reused as sources of raw materials, thereby saving the cost of resources and decreasing the amount of waste production. Their assessments perceived that recycled resources in thermal batteries could decrease virgin materials by a great amount.

Life Cycle Assessment (LCA) of LIB: Conducting life cycle assessments shall be the main objective of evaluating the drawbacks of lithium batteries from production through use to final disposal. Kuo et al., (2022) The research proposes LCA as a tool that can help manage the total emissions for every stage of a battery's lifecycle. Its manufacture and use constitute the need for enhanced recycling practices in the batteries to avoid environmental destruction.

Site Suitability for Recycling Plants: The site for the placement of recycling plants is very important in the quest to maximise the logistics and minimise the emissions associated with transport. Wang et al., (2021) used GIS to evaluate the feasibility of city residents and the location of EV sales for recycling plants of LIBs.

Regulatory Frameworks: Waste management policies must be implemented to assist and promote the sustainable recycling of LIBs. In the work done by Lee et al. (2022), the existing

guidelines regarding the disposal and recycling of batteries are reviewed with strong support for more robust measures to be imposed so that practices within the sector are environmentally friendly.

Recycling Technology Developments: The development of technology in recovering materials from batteries is key to achieving higher recovery rates at a lower cost. In the research done by Y. Zhang et al., (2023) It was reported that biotechnological methods, such as bioleaching and biotechnological hydrometallurgical circuits, are being developed for better recovery of metals from waste and spent batteries.

Interference of the Environment through Ineffective Disposal: The inappropriate management of LIB batteries can have dangerous repercussions on the environment, such as introducing toxic elements to soil and water sources. In a paper published by Patel et al., (2022)The dangers brought by the dumping of waste in landfills are examined, and a call for recycling efforts is made.

Prospective Trends in the Management of Secondary Li-ion Batteries: Markers of current and future literature stress the rapid promotion of the development of management of waste systems for LIBs, which is bound to increase alongside the adoption of EVs. Smith et al., (2023) studied how advanced analytics and machine learning technologies can be incorporated into LIB waste forecasts and decision-making processes.

Regional Characteristics of LIB Recycling: Because of regulations and economies, LIB recycling is approached within each region. Johnson et al., (2022) used a bibliometric approach, where they described those nations that are at the top in the adoption of EVs are also constructing recycling facilities at a steep rate.

2.1 Critical review of literature:

Table 1: Summary of literature reviewed

Title	Authors	Source and Impact Factor	Key Aspects	Summary
The Future of Automotive Recycling: Charting a Sustainable Course (Gaines, 2014)	Gaines, L.	*Sustainable Materials and Technologies* (IF: 10.593)	Discusses global LIB recycling needs, challenges, and future strategies.	Emphasises the importance of early planning for LIB recycling infrastructure and evaluates recycling technologies, such

				as hydrometallurgical and pyrometallurgical methods.
Estimation of EV Waste in the Future and Its Environmental Impact	Zhang, X., Li, W., & Meng, F.	*Journal of Cleaner Production* (IF: 11.072)	Forecasts future LIB waste volumes and examines their environmental implications.	Estimates global LIB waste to exceed 2 million metric tons annually by 2030 and emphasises the role of forecasting models in planning waste management strategies.
Time Series Analysis: Forecasting and Control (G. E. P. Box et al., 2016)	Box, G. E. P., Jenkins, G. M., & Reinsel, G. C.	*Wiley Publications* (Impact: Highly Cited)	Introduces SARIMA and other time series forecasting models, with practical applications.	Provides theoretical foundations and practical guidance for implementing SARIMA, emphasising its suitability for seasonal and non-stationary datasets.
Global EV Outlook 2022(Executive Summary – Global EV Outlook 2022 – Analysis - IEA, 2022.)	International Energy Agency (IEA)	*IEA Report* (Non-Journal; Highly Referenced)	Highlights global EV adoption trends and the corresponding rise in LIB demand and waste.	Projects a tenfold increase in EV adoption by 2030, which will drive LIB demand and waste, and underscores the need for forecasting tools to prepare for this shift.
Challenges and Prospects of Recycling Li-Ion Batteries	Chen, R., Lu, Y., & Yan, Y.	*Nature Sustainability* (IF: 27.157)	Analyzes the challenges in recycling LIBs and presents a framework for	Explores barriers such as cost, technology, and policy and emphasises the importance of integrating

			a circular economy.	forecasting with recycling system design.
Time series analysis and forecasting techniques for municipal solid waste management. (Navarro-Esbrí et al., 2002)	Navarro-Esbrí J, Diamadopoulos E, Ginestar D	*Resources, Conservation, and Recycling* (IF:11.2)	Demonstrates the use of SARIMA for waste forecasting in municipal systems.	Illustrates the reliability of SARIMA in forecasting waste generation and provides insights into seasonal waste patterns applicable to LIB waste forecasting.
Lithium Recovery from Waste LIBs: An Economic and Environmental Analysis	Sun, L., Qi, Z., & Zhang, Y.	*Environmental Research Letters* (IF: 8.985)	Analyses the economic and environmental feasibility of lithium recovery processes.	Concludes that lithium recovery is essential for sustainable LIB waste management and presents cost-benefit analyses to support recycling initiatives.
Improved State-of-health prediction based on an auto-regressive integrated moving average with exogenous variables model in overcoming battery degradation-dependent internal parameter variation (Kim et al., 2022)	Kim S, Lee P, Lee M, Kim J Na W	*Journal of Energy Storage* (IF: 8.9)	Helps in understanding the forecasting methods (SARIMA) model	Highlights the improved accuracy of SARIMA with machine learning models and compares performance metrics like RMSE and MAPE.
Environmental impacts, pollution sources, and	Wojciech Mrozik, ORCID Mohammad Ali	*Energy & Environmental Science* (IF: 39.714)	Explores the environmental hazards posed by LIB waste	Identifies risks such as groundwater contamination and

pathways of spent LIBs (Mrozik et al., 2021)	Rajaeifar, Oliver Heidrichab and Paul Christensenabc		and recycling inefficiencies.	resource depletion and advocates for robust forecasting models to guide recycling and waste management policies.
Critical review of life cycle assessment of LIBs for EVs: A lifespan perspective (Lai et al., 2022)	Lai X, Chen Q, Tang X, Zhou Y, Gao F, Guo Y Zheng Y	*eTransportation* (IF:15)	It gives the EVs waste an environmental footprint, and its impact is calculated at various ecological levels by the LCA approach	This study provides an overview of the framework, methods, and technical challenges of life cycle assessment (LCA), comprehensively reviewing them. This leads to the construction of a cradle-to-cradle LCA framework for LIBs, which analyses carbon emissions during battery production and recycling, as well as under different energy mixes.

2.2. Objectives of the Study:

The present study aims to project LIB waste generation by employing the Seasonal Autoregressive Integrated Moving Average (SARIMA) approach. The SARIMA model is considered a powerful approach to forecasting time series data as it accommodates seasonality, trend, and noise features of the series. Hence, it is ideal for time series data with periodic fluctuations (Box et al., 2015). The authors of this research will, therefore, apply SARIMA to available and historical data for the following purposes:

- To forecast monthly E2Ws sales in India using the SARIMAX time series model based on historical sales data from 2017 to 2024, thereby identifying future market trends through robust statistical modelling.
- To estimate the mass of lithium-ion batteries associated with the forecasted E2Ws sales, using standardised assumptions on battery capacity and specific energy values relevant to dominant battery chemistries (LFP and NMC).
- To project the quantity of EOL LIB waste expected to be generated from E2Ws up to 2030, under three different battery lifespan scenarios (4, 6, and 8 years), simulating real-world battery performance degradation.

To conduct spatial site suitability analysis using GIS-based Multi-Criteria Decision Analysis (MCDA) with Analytic Hierarchy Process (AHP), identifying optimal locations for LIB recycling facilities in Indore district, Madhya Pradesh.

2.3. Scope of the Study:

It is anticipated that the results of this research will enrich the existing literature regarding the potential solutions to handle battery waste. It is important to be able to estimate the volume of LIB waste because:

- Infrastructure Planning: It should enable the designing and sizing of recycling and/or treatment facilities within the existing ones in anticipation of waste generation.
- Policy Making: It can assist governments in regulating the proper disposal or recycling of waste batteries.
- Economic Rationales: It can help increase the recovery of waste materials with primary metals, thus lessening dependence on primary mining.
- Environmental Protection: Mitigating the adverse impacts of LIB waste on ecosystems and public health.

In addition, utilizing the SARIMA approach in this context illustrates how advanced statistical techniques can help overcome issues related to the environment. Machine learning models, for example, are often constrained by overwhelming computational requirements and tedious data preparation processes. SARIMA offers a time series analysis that is simple in application yet effective in results, making it possible for more researchers and practitioners to employ it

2.4. Challenges

Although this study reveals an interesting application of SARIMA for LIBs waste forecasting, there are several challenges. These include:

Limitations of Forecasting into the Future: Effective forecasting hinges on the availability of historical data of sufficient quality, which in some areas may be lacking or incomplete.

Assumptions of Models: For instance, the SARIMA models are based on stationary time series observations, which often necessitate the application of data transformation techniques that may otherwise hinder the interpretation of results.

Change in Context: Technological progress, changes in policies, and economic growth breed uncertainty along time series models as they do not account for such elements.

Notwithstanding these constraints, this study establishes a basic framework for LIB waste forecasting, which is open to improvement with the addition of more predictors and more sophisticated modelling techniques in the subsequent study.

Waste forecasts of LIBs are important in managing waste as well as making waste management strategies effective, as it's limited. Coupled with this, work done by Y. Zhang et al., (2023) stresses predictive models that are required to envisage the amounts of LIB waste at a given point in time, given the expected sales of EVs. The authors employed time series analysis to predict amounts of LIB waste, illustrating this with the evidence that there is a need for precise data in developing strategies for recycling.

Chapter 3

Forecasting Lithium Battery Waste by Two-Wheeler EVs

3. Methodology

This study proposes a systematic, data-driven framework to forecast LIB waste arising from E2Ws adoption in India. The methodology is structured into three interdependent phases: (i) time series forecasting of EV sales, (ii) battery lifespan modelling, and (iii) quantification of EOL LIB waste. Each phase is designed to integrate real-world assumptions and practical constraints in order to produce reliable and policy-relevant waste estimates. A schematic representation of the methodology is provided in Figure 1.

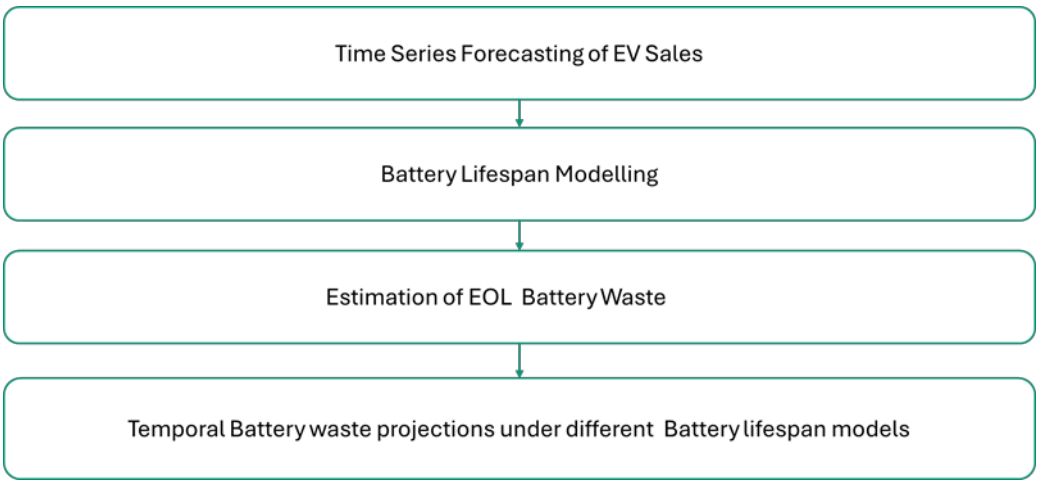

Figure 1: Methodology adopted in this study

3.1. Phase I: Time Series Forecasting of EV Sales:

Accurate forecasting of E2Ws sales is fundamental to estimating the future burden of LIB waste. In this study, historical sales data were used to develop a time series forecasting model based on Seasonal Autoregressive Integrated Moving Average (SARIMA), a widely adopted statistical approach that captures both trend and seasonality in time dependent. This section outlines the data acquisition, preprocessing procedures, model development, and validation methodology adopted in Phase I.

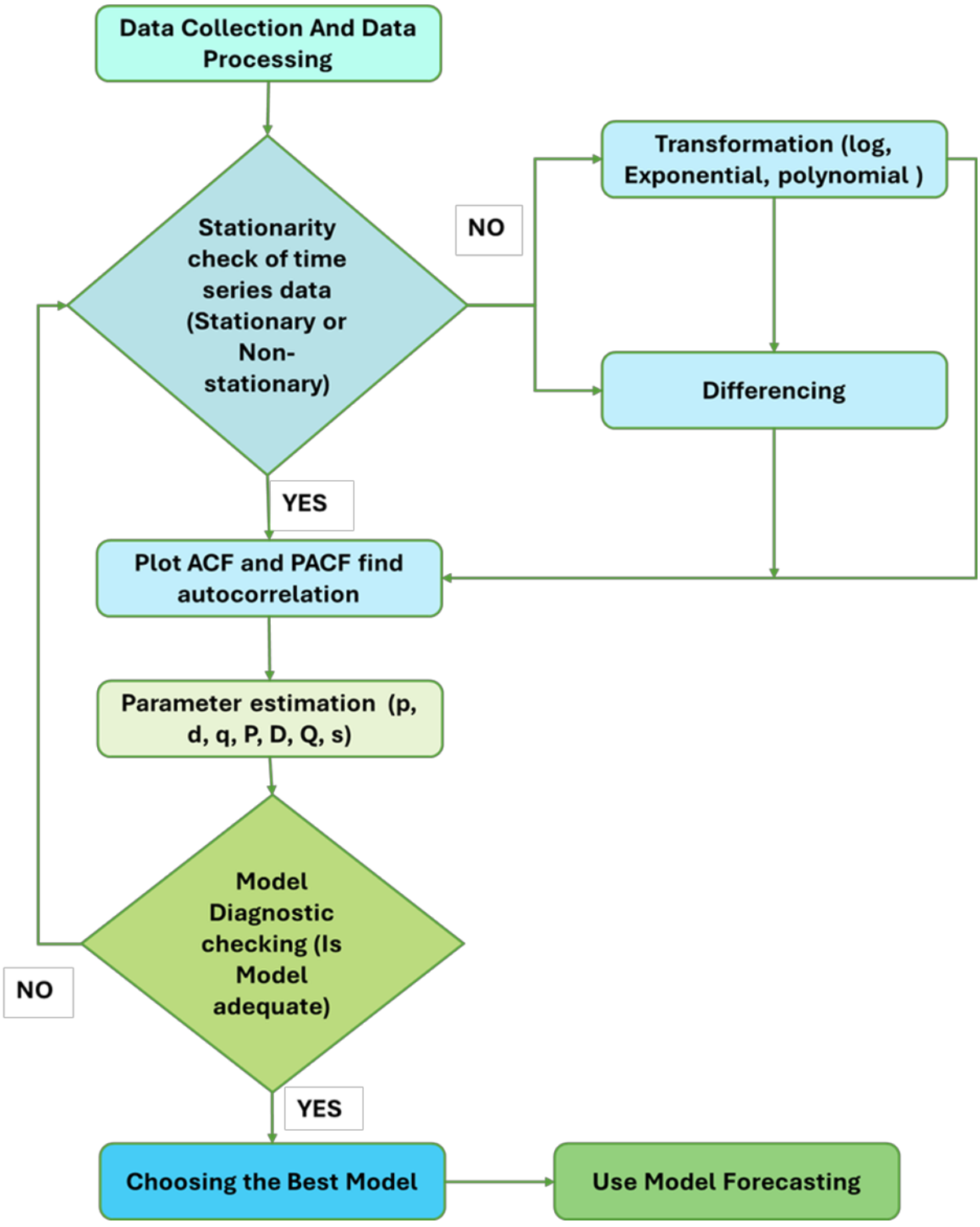

Figure 2: SARIMA model methodology

3.1.1. Data Collection

The main data source is the **VAHAN portal (https://parivahan.gov.in/parivahan/)** from the Ministry of Road Transport and Highways, Government of India, which provides authentic registered vehicle data. Monthly sales data of electric E2Ws in India were collected for the

period ranging from January 2017 to October 2024. The data collected for this study include the different classes of E2Ws, such as M-Cycle/Scooter, M-Cycle/Scooter-With Side Car, Moped and Motorised Cycle (CC>25cc), as classified in the Vahan Portal. Further, the data from these classes of two-wheelers have been aggregated and collectively referred to as E2Ws for the purpose of forecasting future sales. For the visualisation of the sales data, the plot is provided in Figure 3. Table 1 shows the units sold over the course of a year.

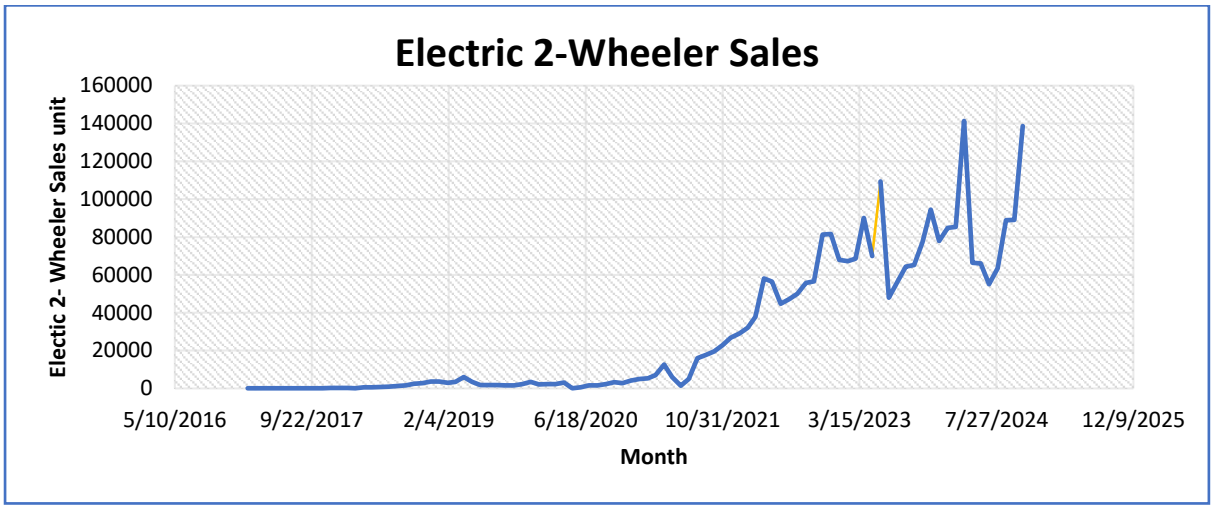

Figure 3: Monthly E2Ws sales plot

3.2 Data Preprocessing:

To process the data for time series modelling, Standard data processing procedures were followed. First, the dataset was searched for missing values and outliers. . The data was then dated-indexed and resampled to maintain a uniform monthly frequency. In this research, real-life monthly sales figures of E2Ws available in India from January 2017 to October 2024 were used. The data showed significant non-stationarity and seasonality, which were handled by second-order differencing and seasonal decomposition. To identify potential anomalies within the dataset, the Z-score method was applied.

The Z-score is computed as: $Z = \frac{Value - Mean}{Standared\ Deviation}$

Data points with a Z-score exceeding +3 or falling below -3 were considered statistical outliers. These pre-processing techniques were necessary to make the data conform to SARIMA modelling assumptions and to improve the accuracy of forecasts

Table 2: Electric two-wheeler monthly sales data

Month/ Year	Jan	Feb	Mar	April	May	June	July	Aug	ep	Oct	Nov	Dec
2017	110	81	146	97	94	136	119	107	117	167	236	195
2018	199	171	518	524	698	1010	1297	1587	2382	2847	3633	3568
2019	2929	3493	6003	3547	1755	1814	1727	1645	1673	2241	3425	2057
2020	2373	2286	3063	91	584	1600	1632	2324	3367	2764	4214	4931
2021	5375	6961	12539	6043	1430	5031	16004	17717	19608	22871	26845	28986
2022	32006	37874	58056	56376	44669	47097	49990	55701	56612	81280	81560	67910
2023	67313	68601	90093	69921	109383	47911	56139	64311	65149	77208	94514	77873
2024	84762	85267	141328	66408	66103	55092	63576	88878	89037	138591		

3.2.1. Exploratory Data Analysis (EDA):

From the visual inspection of the Monthly E2Ws sales dataset plot in Figure 3, sales figures for electric E2Ws in India between January 2017 and October 2024 were inspected to understand underlying patterns and trends. The pattern of E2Ws sales exhibits a distinct exponential increase from the end of 2020. It is then a phase transition from a basically flat and idle phase to an accelerating rise trend in volume sales. We can also observe the impact of COVID-19 on the sales figures in April 2020, a sudden drop in sales; however, following that, a visible upward trend began to emerge.

Moreover, the series exhibits large seasonal variations—periodic drops and spikes—pointing towards a possible effect of seasonal or policy-related factors on consumer purchasing behaviour. Some evident sudden spikes in sales also indicate the existence of external shocks, e.g., policy shifts, subsidies such as FAME Phase I and FAME Phase 2 programs by the Government of India and supply chain events(Electric Vehicles: Electric Vehicle Industry in India and Its Growth, 2021.-b).

This preliminary analysis confirms that the data is non-stationary and contains both trend and seasonal aspects. From this initial inspection and data pattern analysis, it helps to identify and

select an appropriate time series model, thereby establishing the necessity of differencing and seasonal modelling procedures like SARIMA for efficient forecasting.

3.2.2 Seasonality and trend analysis:

To detect seasonality and trend in time series data, both STL (seasonal-trend decomposition using losses) and classical Decomposition techniques were used (Wen et al., 2019). These methods allowed us to deconstruct the time series data into its core components- trend, seasonality and residuals, facilitating a clear understanding of underlying patterns (Bandara et al., 2025). From the STL decomposition, we can understand a robust, noise-resistant view of seasonal behaviour, while the classical method validated its consistency across time. The results from both decompositions provided strong evidence of a repeating annual pattern, justifying the incorporation of seasonal components into the forecasting model. Based on these insights, a Seasonal ARIMA (SARIMA) framework with a 12-month periodicity and seasonal differencing (D=1) was selected for further modelling and evaluation.

3.2.3 Tests of Stationarity and Differencing

Before applying the SARIMA model for time series data one of the basic assumptions are made, that is data should be stationary, and it is necessary in the series and should be tested for stationarity to check the stationarity of the time series data the Augmented Dicky fuller test is performed.

- **Augmented Dickey-Fuller (ADF) test**

Making time series data stationary is an important requirement for time series forecasting. This ensures that the statistical properties (mean, variance, and autocorrelation) associated with the data remain unchanged over time, allowing predictions to be accurate Manuca & Savit, (1996). The Augmented Dickey-Fuller (ADF) test is performed to check for stationarity in the time series data. A high p-value (> 0.05) indicates no stationarity, so data transformation is required. Differentiation is the most common method of removing trends and seasonality from a time series. The first differencing is calculating the difference between two consecutive data points. It removes linear trends and partially stabilises the variance. If still present, for residual trends or seasonality, second differencing can be applied, as this will stabilise variance further, producing a zero-mean series. ADF tests are repeated at each stage to confirm the succeeding stationary condition. Stationarity means the model captures stable relationships, which are valid for predicting EV sales and the output of LIB waste generation. Proper preprocessing, like differencing, improves the extent to which time series models can be relied on.

The ADF test examines the presence of a unit root in the series by evaluating whether the null hypothesis of non-stationarity can be rejected (Paparoditis & Politis, 2018). A low p-value (typically less than 0.05) suggests the series is stationary, allowing model fitting without additional differencing; otherwise, differencing is required to stabilise the mean. In SARIMA modelling, the ADF test is typically applied before model specification to determine the order of non-seasonal differencing (d) and, when used in conjunction with seasonal decomposition, informs the need for seasonal differencing (D). The ADF test output includes the test statistic, critical values, and p-value, and is implemented using statistical software such as Python's stats model's package. Identifying the correct level of differencing through the ADF test ensures the time series meets the stationarity condition, improving the accuracy and reliability of SARIMA-based forecasts.

3.2.4 SARIMA Model Overview:

The SARIMA model is a modified version of the ARIMA model with an added focus on seasonality. It applies primarily to time series data that can be observed as having a definite trend and a cyclical data pattern (seasonality). The SARIMA model is the Extended version of ARIMA, first introduced by Box and Jenkins in 1970 as part of the broader Box-Jenkins methodology for time series forecasting (G. Box, 2013). Their work laid the foundation for modelling non-stationary seasonal data using autoregressive and moving average structures and remains one of the most influential contributions to time series analysis.

SARIMA model structure

The following notation is used to express the elements of the SARIMA model:

$$\Phi_P(B^S)\phi_P(B)(1-B)^d(1-B^S)D_{y_t} = \Theta_Q(B^5)\theta_q(B)\epsilon_t \quad \text{Eq1}$$

Where,

Non-seasonal components:

$\Phi_P(B)$: Non-seasonal autoregressive polynomial of order p.

$(1-B)^d$: Non-seasonal differencing of order d.

$\theta_q(B)$: Non-seasonal moving average polynomial of order q.

Seasonal components:

$\Phi_P(B^S)$: Seasonal autoregressive polynomial of order P.

$(1-B^S)^D$: Seasonal differencing of order D and seasonality s.

$\Theta_Q(B^S)$: Seasonal moving average polynomial of order Q.

Other terms:

B: Backwards shift operator

s: Seasonality period.

ϵ_t: White noise error term.

3.2.5 SARIMA Model Parameters and Their Identification

- **Non-Seasonal Parameters (p, d, q):**

Autoregressive order (p): the number of lag observations (previous values) included in the model to forecast the current value. In other words, it explains how many past observations the current value of the time series will be for the forecast. The value of p is established from the behaviours of the Autocorrelation Function (ACF) and Partial Autocorrelation Function (PACF) graphs.

Differencing order (d): This factor specifies how often the time series should be differenced to achieve stationarity, that is, to eliminate trends or seasonal patterns in the data. Differencing the data helps in mitigating seasonality and trends. It is typical to try d=1 first and see whether one can get the series stationary using the ADF test.

Moving Average order (q): This parameter states the number of lagging forecast errors in predicting future values. It denotes the lagged average of past forecast error (prediction value minus actual value), which affects the current value. Like p, q is determined using ACF and PACF plots.

- **Seasonal Parameters (P, D, Q, s):**

Seasonal Autoregressive Order (P): The contribution of past seasonal observations to the current value of the time series is analysed in this seasonal lag and hence comes in a similar order with the inclusion of p, but not as P. The degrees of P are assigned accordingly to the calendar in the series under consideration.

Seasonal Differencing Order (D): It is often necessary to include seasonal differencing to stabilise the time series. Suppose the data display seasonality without such a fixed nature (i.e., it shows an upward or downward trend, a seasonal repetition of patterns). In that case, this sort of differencing can be performed to mitigate such seasonal variations in trends. The limit of values for D usually varies from 0 to 1.

Seasonal Moving Average Order (Q): This is the total number of seasonal forecast error metrics that were lagged and included in the model. It is almost identical to q, but concerning the temporal aspect of the time series. This tail end of the hybrid equation combines previously

measured season forecast errors, contributing instead of being a standalone measurement, as in the non-seasonal case.

Seasonal Period (s): This is the time taken to complete one seasonal cycle and represents the frequency at which the seasonality is repeatable in the data. To illustrate in year data, the seasonal period might be *s=12* if the data in question is monthly, such that one cycle takes 12 months. If the data in discussion is daily, then s=7, some might say that seasonality is in weeks.

3.2.6 Diagnostic Checking

Diagnostic checking is performed to evaluate the adequacy and validity of the model. These checks are essential to ensure that the residuals, representing the portion of the data not explained by the model, resemble white noise. This indicates that the model has effectively captured the underlying structure of the time series.

Initially, the residuals were subjected to visual inspection using a histogram and the kernel density estimation (KDE) plot to assess their distribution. Ideally, the residuals should follow a normal distribution, evidenced by a bell-shaped and symmetric curve. This was further supported by the Q-Q (quantile-quantile) plot, which compares the quantiles of a normal distribution. A good fit is indicated when the residuals lie approximately 45-degree reference line.

Secondly, the autocorrelation of residuals was evaluated using the Autocorrelation function plot, also known as the correlogram. For a well-specified SARIMA model, the residuals should not exhibit significant autocorrelation. In this study, the majority of the ACF spikes fell within the 95% confidence interval, suggesting that the residuals, suggesting that the residuals are largely uncorrelated.

In addition to the graphical methods, statistical tests were applied to reinforce the findings. The Ljung-Box test was employed to examine whether the residuals are independently distributed. Furthermore, the Jarque-Bera test was conducted to assess the normality of residuals. The resulting p-values supported the assumption of normal distribution. Lastly, the results indicated a relatively constant variance over time, supporting the model's assumption of homoscedastic errors.

Overall, these diagnostic checks confirm the adequacy of the SARIMA model by ensuring that the residuals exhibit the characteristics of white noise, thereby validating the model's suitability for reliable forecasting

3.2.7 Model Training and Validation

To evaluate the predictive performance of the SARIMA model, the available time series data were divided into subsets: the training set and the testing set. The training set, consisting of the initial portion of the dataset, was used to fit the SARIMA model and estimate its parameters. The remaining data comprised the testing set, which was reserved for out-of-sample testing validation. Model forecasts generated from the training data were compared against the actual observed values in the testing set. This approach allows for the evaluation of the model's generalisation ability and helps to avoid overfitting. Common accuracy matrices such as Mean Absolute Error (MAE), Root Mean Square Error (RMSE), Mean Absolute Percentage Error (MAPE), and R^2 were employed to quantify the forecasting performance. A lower value of these matrices indicates better model accuracy. this validation step is crucial to ensure that the selected model performs reliably when applied to future data. To perform the above approach, the SARIMAX function from the statsmodels Python package was used using various combinations of parameters, the optimal of which was selected based on the Evaluation matrix results on the testing set.

3.2.8 Metrics for Model Evaluation

1. Root Mean Square Error (RMSE):

Measures the square root of the average squared differences between predicted and actual values.

Formula: RMSE = $\sqrt{\frac{1}{n}\sum_{i=1}^{n}(y_i - \bar{y})^2}$

Interpretation: Smaller values indicate better performance. RMSE is sensitive to outliers because of the squared term.

2. Mean Absolute Percentage Error (MAPE):

Measures the average percentage error between actual and predicted values.

Formula: MAPE $MAE = \frac{100}{n}\sum_{i=1}^{n}|y_i - y_o|$

Interpretation: MAPE values below 10% are considered excellent, 10-20% good, and above 30% indicate poor performance(Montaño Moreno et al., 2013).

3. Mean Absolute Error (MAE):

Measures the average magnitude of the errors without considering their direction.

Formula: $MAE = \frac{1}{n}\sum_{i=1}^{n}|y_i - y_o|$

Interpretation: MAE is less sensitive to outliers compared to RMSE.

4. Coefficient of Determination (R^2):

Measures how much of the variance in the actual data is explained by the model.

Formula: $R^2 = 1 - \frac{\sum_{i=1}^{n}(y_i - y_\infty)^2}{\sum_{i=1}^{n}(y_i - \bar{y})^2}$

Interpretation: R^2 values range from 0 to 1, where higher values indicate a better fit. Negative values indicate the model performs worse than a simple mean or mode.

3.3 Phase II: Battery Lifespan Modelling

Battery lifespan modelling is critical for accurately estimating the volume/mass of the battery that will retire after serving a particular time. Battery lifespan refers to a lithium-ion cell's operational duration, typically measured by its cycle or calendar life (Jaguemont et al., 2016). Cycle life denotes the total number of complete charging and discharging processes the battery can sustain before its performance drops below an acceptable threshold(Z. Zhang et al., 2022) and the timeline of lithium-ion batteries (LIBs) reaching EOL, which forms the basis for waste forecasting and circular economy planning. The estimation of the LIB life span is crucial. The exact life span of a LIB estimation is challenging due to the influence of multiple factors that impact the life span of EV batteries, such as temperature, charge-discharge cycle, user behaviour and Overcharge and Over-discharge (X. Zhang et al., 2021).

In this study, the battery lifespan refers to the operational period during which a battery retains acceptable performance in its primary application—E2Ws—before degrading to the point of replacement. In practical life, lithium-ion batteries used in EVs are retired after use, reaching 80% of their nominal capacity (J. Zhang et al., 2024). Previously, some studies have assumed a calendar life of the lithium-ion battery, which is used to power EVs, ranging between 8 and 10 years (Englberger et al., 2019; Maisel et al., 2023; Yang et al., 2024). Additionally, Ai et al. (2019) compiled findings from multiple sources, reporting LIBs' lifespans varying from as low as 3 years to as high as 16 years. Depending on operational and environmental conditions. Based on these prior works, many researchers adopt a maximum functional lifespan of 10 years as a standard assumption for EV Battery performance. This study employs a time-lag-based deterministic model wherein each battery is assumed to be retired after a predefined lifespan. On the safer side, to maintain a conservative and realistic estimate, we assume a battery life

span that typically ranges from 4 to 8 years, depending on usage intensity, ambient temperature, charging behaviour, and battery chemistry employed.

According to the Global EV Outlook reports IEA, 2023 most commonly used lithium-ion chemistries in EV drives are Lithium Iron Phosphate (LFP) and Nickel Manganese Cobalt Oxide (NMC), which dominate the market due to their energy density stability and performance, which translates into a lifespan of 4–8 years under real-world conditions. Based on literature and market practice, this study models three lifespan scenarios: short (4 years), base (6 years), and long (8 years), assuming 100% LIB penetration in E2Ws. The number of batteries reaching EOL in a given year is estimated by shifting the SARIMA-forecasted E2Ws sales forward by the assumed lifespan.

The following formula gives the battery retirement count for year t:

$$EoL_t = \sum_{1=1}^{n} \left(S_{t-L_i} \times (1 - R_i) \right) \quad \text{Eq. 2}$$

Where:

EoL_t: Number of batteries reaching EOL in year t

S_{t-L_i}: Number of E2Ws sold in the year $t - L_i$

Li: Assumed lifespan of the battery (years)

Ri: Second-life or reuse rate (fraction of batteries not contributing to immediate waste)

n: Number of lifespan scenarios considered (e.g., 3 for 4, 5, 8 years)

- This model assumes each vehicle sold in year $t-L_i$ will result in one LIB reaching EOL in year t, adjusted for any reuse rate R. If reuse is excluded (i.e. R=0), the formula simplifies to $EoL_t=S_{t-L}$.
- The output of this phase is a timeline of retired battery quantities (units/year), which directly feeds into the waste quantification phase, where the total battery mass (kg) and energy capacity (kWh) are estimated.
- The retirement year for each cohort of sold vehicles was determined as:
- Retirement Year=Sales Year + Battery Lifespan

3.4 Phase III: Estimating End-of-Life Battery waste from the sales of Electric E2Ws Vehicles.

3.4.1. Formulation of Battery waste:

Total Energy Used in Month m of Year t: The total energy required for the EVs sold in month m of year t is:

$E_{m,t} = S_{m,t} \times C$

$E_{m,t}$ Is that the month's total energy consumption in kWh?

Battery Waste Generated in Month m of Year t: The total weight of LIB waste generated in month m of year t is:

$$Wm,t = \frac{(Em,t \times C)}{SE\left(\frac{kWh}{kg}\right)} \quad \text{Eq. 3}$$

$$\text{Where } (W_{total})annual = \sum_{n=1}^{12} \frac{S_{m,t} \times C(kWh)}{SE\left(\frac{kWh}{kg}\right)} \; or \; \sum_{h=1}^{12} w_{m,t} \quad \text{Eq. 4}$$

Where:

- $W_{m,t}$ = the total potential battery waste (in kg) for month m of year t.
- W_{total} = Total battery waste (kg) over n months
- $S_{m,t}$ = Forecasted and past sales for month m of year t
- C = Battery capacity per EV (kWh)
- SE = Specific energy of battery (Wh/kg)
- T = Number of years

3.4.2. Average battery Capacity(C) Estimation:

The estimation of the average battery capacity required for E2Ws in this study is based on data presented in the ICCT (International Council on Clean Transportation) Working Paper *(*Gode et al., 2021). This report offers comprehensive insights into the battery capacity of various E2Ws models in the Indian market. By referencing the net battery capacities of E2Vs and utility/multi-purpose vehicles, ranging from 0.3 kWh in entry-level models to 9.7 kWh in premium variants, I derived average capacity and vehicle categories. This value serves as a representative and realistic benchmark for modelling battery demand and evaluating future requirements in India's dynamic and rapidly expanding electric mobility sector.

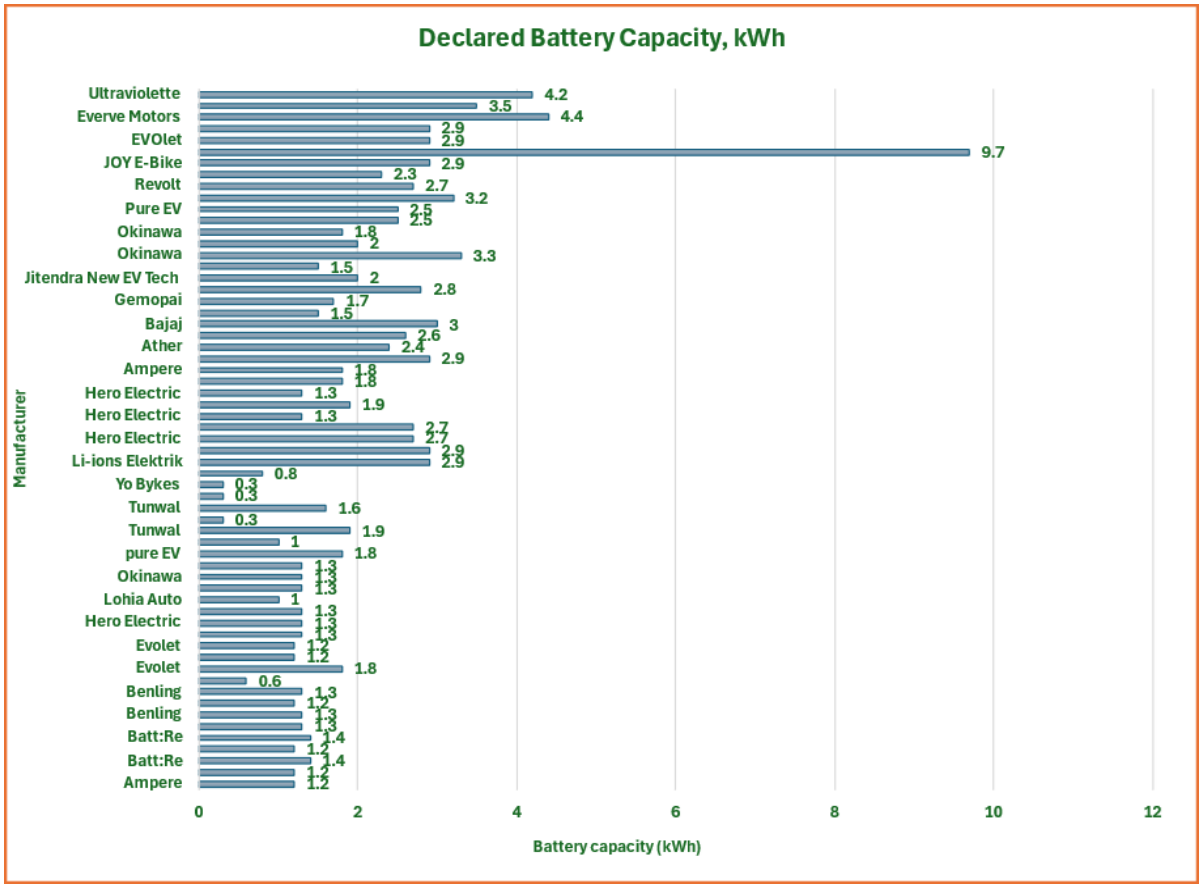

Figure 4: Battery capacity of different types of E2Ws sold in India

3.4.3 Battery Specific Energy (Wh/kg)

Common LIB Chemistries in EVs**:** Lithium-ion batteries (LIBS) are the dominant energy storage technology in EVs due to their high energy density, long cycle life, and decreasing costs. Among the various LIB chemistries, the following are most widely used in modern EVs:

- **Nickel Manganese Cobalt Oxide (NMC):** Known for its balanced energy density, power output, and thermal stability. Variants like NMC622 and NMC811 are widely used by manufacturers such as BMW and Hyundai (Tallman et al., 2021).
- **Nickel Cobalt Aluminium Oxide (NCA):** Offers higher energy density compared to NMC and is commonly used in Tesla vehicles. However, it is less thermally stable than LFP.
- **Lithium Iron Phosphate (LFP):** Provides excellent thermal stability and long cycle life at a lower cost, though with lower specific energy. It is increasingly adopted in EVs targeting affordability and safety, such as those from Tata Motors and BYD.

The mass of LIB waste from the EOL EVs was estimated through the reverse-calculation approach based on rated battery capacity and cell-level specific energy density. Through the estimation of cell mass entering the waste stream, which is critical for assessing recycling potential and planning infrastructure. Current commercial lithium-ion cells using nickel manganese cobalt (NMC) and nickel cobalt aluminium (NCA) technologies demonstrate specific energy levels ranging from 220 to 260 Wh/kg. In contrast, lithium iron phosphate (LFP) cells typically have specific energy values between 150 and 160 Wh/kg. The specific energy and energy density of these batteries have more than doubled compared to the original designs, which had a specific energy of just 120 Wh/kg (Frith et al., 2023). Similarly, Schmuch et al., (2018) reported specific energy NMC 622/811 cells with 230–250 Wh/kg, and LFP chemistry around 160 Wh/kg. These values are further supported by Liao et al., (2024) which show energy densities of 200 Wh/kg for cylindrical NCA cells and around 163 Wh/kg for LFP prismatic cells.

In this study, a foundation assumption established a base case scenario with specific energy of 210 Wh/kg; which serve as the cornerstone for all subsequent battery mass calculation This representative average was derived by taking the midpoint between lower bound of 160 Wh/kg and the upper bound 260 Wh/kg, taking into account the two most widely LIB chemistries, LFP and NMC. IT is important to note that this specific energy estimate applies strictly to the cell mass only, excluding other battery pack components**.** All the estimations concerning battery cell mass throughout this study are based on this benchmark case scenario. This methodological approach is critical not only for accurately modelling battery material flow analysis (MFA) but also for projecting future recycling volumes. It also aids in informing infrastructure planning and development for battery retirement management after they have completed their life cycle services. By anchoring the analysis to standardised and representative energy density, the study ensures consistency, relevance, and scalability in assessing material and energy flows across the LIB value chain.

Chapter 4

Site Suitability Analysis for the LIB Recycling Plant for Indore City

4.1 Study Area:

This Study focuses on the part of Indore city located in the Indore district of Madhya Pradesh, India, which falls under the geographical coordinates of nearly 22^0 43' N latitude and 76^0 42'E longitude and 1805 feet above MSL (mean sea level)(Goyal, 2011). It lies on the Malwa Plateau and is linked by national highways, railways, and air transport, making it the ideal logistics and industrial hub of central India (Kumar et al., 2007), (Verma & Bhonde, 2014). Indore has been ranked as the cleanest city in India for the sixth consecutive year under the Swachh Survekshan mission from 2017 to 2023, marking strong urban management and civic participation.

Indore's climate is considered to be semi-arid, with hot summers, monsoon season from June to September, and cool, dry winters (Kawadia & Tiwari, 2017). This sort of climatic condition is generally quite appropriate for industrial operations, including the handling and processing of LIB waste, which is susceptible to extreme environmental changes.

Indore has logistics and environmental planning advantages for setting up a LIB recycling plant site. The city has several industrial areas, such as the Sanwer Industrial Area, Pithampur Industrial Area, and, lastly, the emerging Super Corridor, in addition to these potential zones for industrial development, all plus the existing utility networks. Added to this are the advantages of the major EV markets' proximity and pre-existing solid waste infrastructure, which include the Indore Integrated Solid Waste Management Plant, besides growing Clean Energy initiatives' ecosystem to solidify the case for the study.

This study brings in the site suitability analysis concerning a wide variety of geospatial and environmental parameters using the GIS-based multi-criteria decision analysis (MCDA) framework. The factors under consideration include land use/land cover, proximity to transportation networks, distance from residential zones, groundwater sensitivity, and slope. Satellite imagery, municipal land use maps, and field verification were used to create spatial data for these layers. The model used is a weighted overlay to identify those optimal locations for Indore's urban and peri-urban areas where recycling plants could be located.

A base map of Indore has been prepared using GIS software (QGIS/ArcGIS), which delineates study boundaries and thematic layers used for spatial analysis (Figure 5). It supports the geospatial approach to evidence-based decision-making in sustainable infrastructure planning for the emerging EV ecosystem.

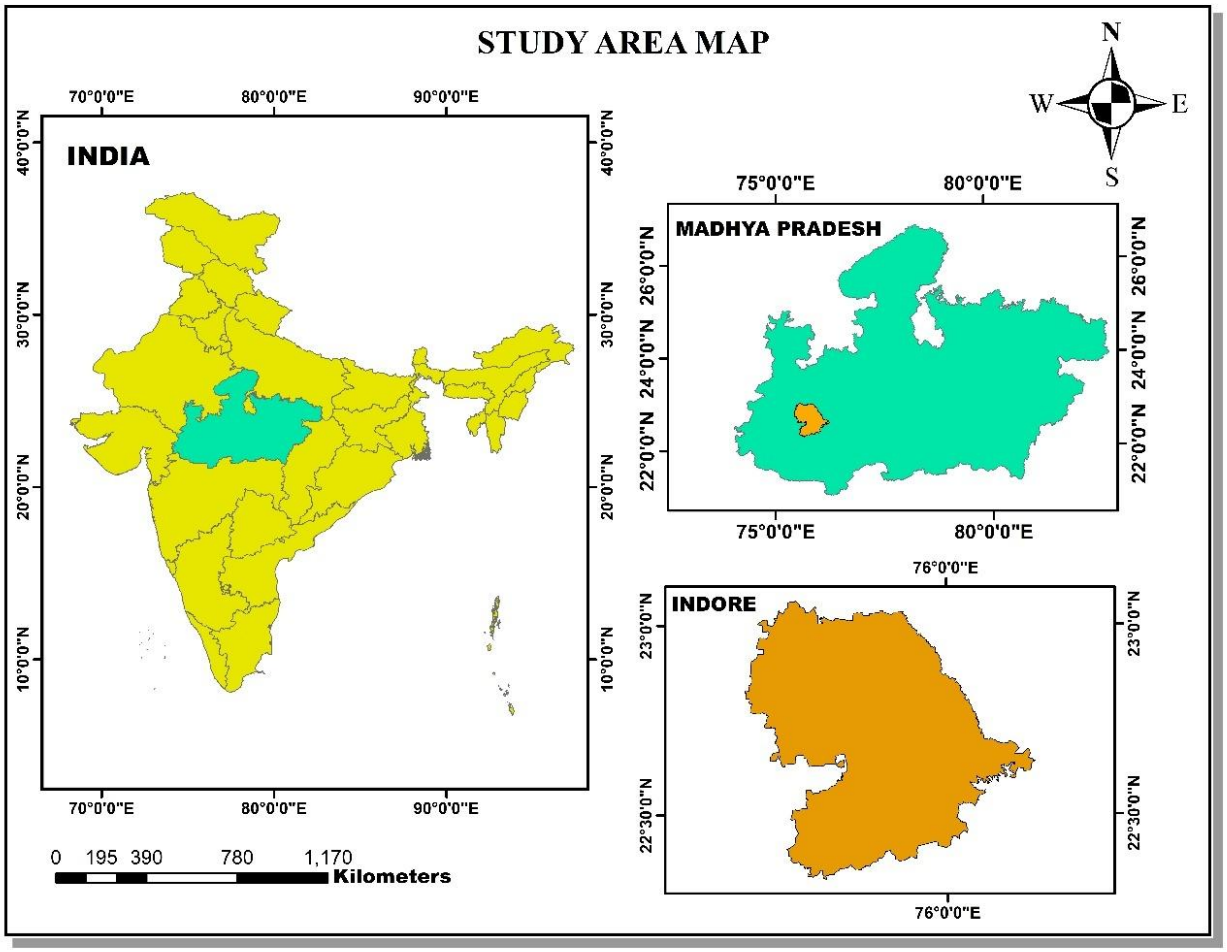

Figure 5: Study area map for the LIB recycling plant

4.2. Methodology:

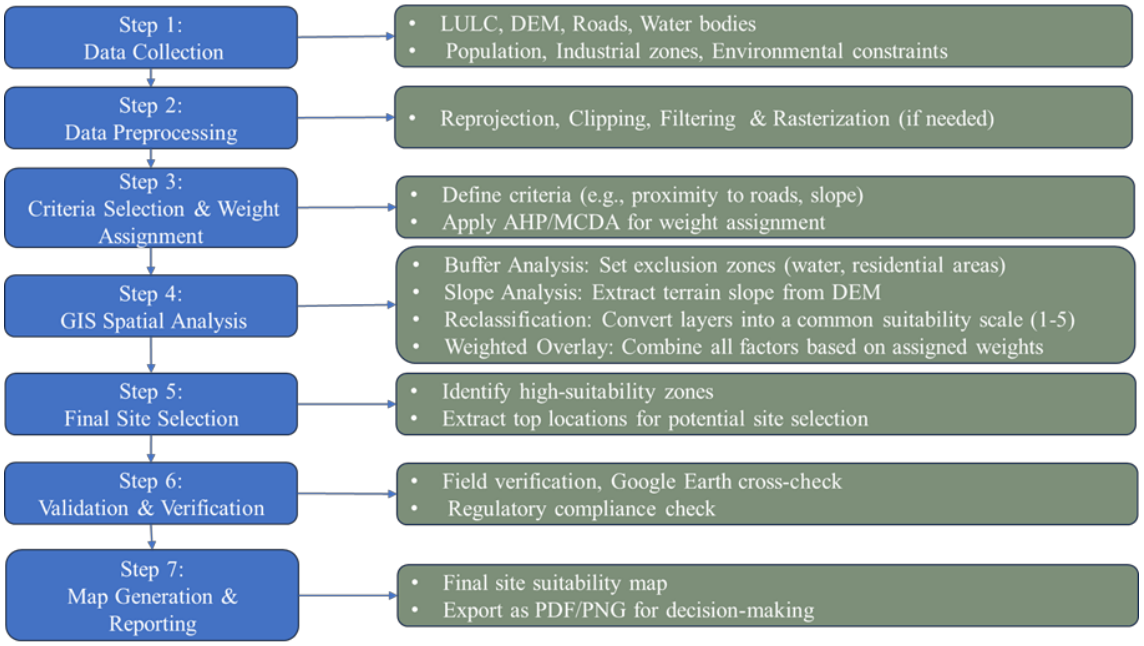

Figure 6: Flow chart for site suitability analysis

4.2.1. Data Collection:

The study is conducted in **Indore, Madhya Pradesh,** a rapidly growing urban centre with increasing EVs adoption and lithium-operated battery consumer Electronics. The present study utilised a range of spatial and non-spatial datasets to conduct a site suitability analysis for the establishment of a LIB recycling plant in Indore district, Madhya Pradesh, India. The administrative boundary shapefile for Indore district was obtained from the **Survey of India**, which provided the geographic extent for the study area and served as a base layer for spatial analysis.

The following datasets were collected, which include Primary as well as secondary sources:

Table 3: Inventory of spatial data layers and corresponding data sources

Sl No.	Spatial Layers (GIS format)	Data Source
1	India, Madhya Pradesh and Indore District Shape File	Survey of India
2	Land Use/Land Cover (LULC) map (10M resolution)	Esri Sentinel-2
3	Road network	Open Street Map
4	River	Open Street Map
5	Slope and elevation (DEM)	https://earthexplorer.usgs.gov
6	Industrial Area	Open Street Map
7	Surface Water Bodies	Landsat and Sentinel using Google Earth Engine and OpenStreetMap

The Shuttle Radar Topography Mission (SRTM) Digital Elevation Model (DEM) provides near-global elevation coverage between 60°N and 60°S, including the entire Indore district in Madhya Pradesh, India. The DEM tiles, available in 5° × 5° extents and referenced to the WGS84 geographic coordinate system, were mosaicked to create a seamless elevation surface for the study area. Using the Spatial Analyst tools in ArcGIS software, a slope map was derived from the DEM.

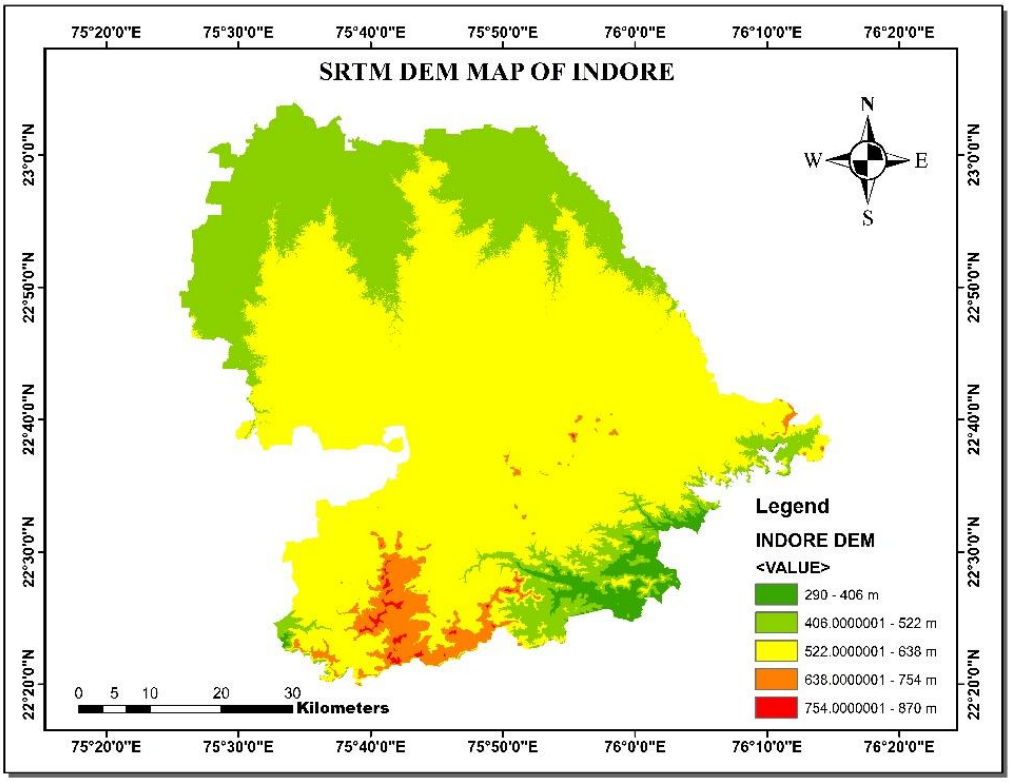

Figure 7: SRTM DEM map of Indore district

SRTM data were collected during NASA's 11-day STS-99 mission in February 2000 by a specially modified radar system onboard the Space Shuttle *Endeavour*. This system was based on the earlier Spaceborne Imaging Radar-C/X-band Synthetic Aperture Radar (SIR-C/X-SAR) technology. The SRTM DEM, with a spatial resolution of 30 meters (1 arc-second), was utilised in this study, which served as essential input parameters in the Analytical Hierarchy Process (AHP)-based site suitability analysis for identifying optimal locations for LIB recycling in the Indore district.

Land use and land cover (LULC) information was extracted at 10m resolution for the year 2024 from Esri Sentinel-2 imagery, which offers high-resolution satellite data suitable for classifying

built-up areas, vegetation, barren land, and other surface types. This LULC data provided insights into existing land utilisation and helped in identifying potential sites with minimal environmental disruption.

Additional thematic layers—including roads, rivers, and industrial areas—were sourced from OpenStreetMap (OSM) and processed using QGIS. These layers were used to assess the proximity of candidate sites to essential infrastructure such as transportation networks and existing industrial zones, as well as to evaluate potential environmental constraints related to water bodies.

4.2.2. Software Used:

Quantum GIS 3.36- QGIS is a robust, free, and open-source desktop Geographic Information System (GIS) application that provides users with comprehensive tools for viewing, editing, and analysing geospatial data. It supports a wide range of data formats and allows for extensive customization through plugins. QGIS is compatible with multiple operating systems, including Windows, macOS, and Linux, making it accessible to a diverse user base.

ArcGIS - The ESRI Software Company developed this software, which is not free. ArcGIS Desktop is a comprehensive desktop GIS software suite that enables users to create maps, conduct spatial analysis, and manage data. All layers are defined using this software.

Google Earth Engine (GEE) – GEE is a cloud-based platform used in this study for processing and analysing satellite imagery. It provides access to a large repository of geospatial datasets, such as Landsat and Sentinel, and supports fast, large-scale analysis through cloud computing.

4.2.3. Criteria Selection for Site Suitability

The selection of appropriate criteria is a critical step in the site suitability analysis for industrial infrastructure, particularly for environmentally sensitive facilities such as LIB recycling plants. In this study, six spatial criteria were identified based on their relevance to environmental, technical, and logistical feasibility. These criteria were selected through a review of existing literature, expert knowledge, and alignment with regulatory and planning guidelines. The selected layers include Land Use and Land Cover (LULC), proximity to industrial areas, surface water bodies, road networks, and slope**,** each of which plays a significant role in determining the suitability of a site. The Analytical Hierarchy Process (AHP) was employed to assign relative weights to these criteria and integrate them into a comprehensive multi-criteria decision-making framework.

The following six criteria were selected for AHP-GIS analysis in Table 4.

Table 4: Criteria-based Thematic Layers Selection

Criterion	Justification
Settlements (LULC)	To reduce health/safety risks
Proximity to roads and rail	For transportation/logistics
Land use compatibility (industrial zones)	Legal and operational feasibility
Distance from water bodies	To prevent water pollution
Slope/elevation	Site engineering feasibility
River	To ensure environmental protection

4.2.4. Analytical Hierarchy Process (AHP)

The Analytic Hierarchy Process (AHP) is one of the multi-criteria decision-making methods that was originally developed by Prof. Thomas L. Saaty(R. W. Saaty, 1987). The procedure of AHP can be divided into three parts, which include identifying a hierarchy of objectives, criteria and alternatives; pairwise comparison of criteria; and integration with the results from pairwise comparison as relative importance over all levels of the hierarchy. This method is used to determine the percentage importance of the parameters used in the identification of suitable sites for. The integration of AHP with GIS gives an efficient and user-friendly way for solving complex problems, as it is a combination of decision-making support methods and tools with powerful capabilities of mass data computation, visualisation, and mapping(Chandio et al., 2013). The implementation of AHP can be summarized as following procedure: definition of objective; identification of criteria; data collection and preprocess; digitization of criteria and convert all data into vector data; classification of raster datasets; creation of preference matrix; determination of criteria weights according to calculation based on preference matrix; weighted summation of criteria raster datasets as result(Kaya et al., 2022),(Ifg, 2017.). The AHP procedure involves performing the comparison of pairs of parameters within a set of reciprocal matrices in comparing pairs of factors(T. L. Saaty, 2005). The AHP scale of relative importance is used on a scale of 1 to 9(T. L. Saaty, 2014), as shown in Table No. 5. Based on a literature review of previous studies, specific conditions of Land Suitability analysis, 6 criteria considered as main factors are chosen for this study, including: Topographic conditions (Slope), Industrial Area, LULC, RIVER, Road Network, and Surface Water Bodies.

Table 5: Hierarchy structuring based on importance scale

VALUE	SIGNIFICANCE
1	Equal importance
3	Moderate importance of one over the other
5	Strong importance
7	Very strong importance
9	Extremely strong importance

The pairwise comparison matrix for criteria, denoted by C, is structured as follows:

$$C = \begin{bmatrix} 1 & a_{12} & a_{13} & \dots & a_{1n} \\ 1/a_{12} & 1 & a_{23} & \dots & a_{2n} \\ \vdots & \vdots & 1 & \vdots & \vdots \\ \vdots & \vdots & \vdots & 1 & \vdots \\ 1/a_{1n} & 1/a_{2n} & 1/a_{3n} & \dots & 1 \end{bmatrix}$$

where a_{ij} represents the relative importance of criterion i compared to criterion j.

The matrix is reciprocal, meaning $a_{ij} = 1/a_{ji}$

- **Criteria Selection Description:**

Table 6: Classification and suitability scale

	Reclassification	Suitability scale
Distance from major roads	<250 m	1
	250-750 m	5
	750-1500 m	4
	1500 -2000 m	3
	>2000 m	2
Surface water Body	<250 m	1
	250-500 m	2
	500-1000 m	3
	1000-4000 m	4
	>4000 m	5
River/streams	0-500 m	1
	500-1000 m	2
	1000-2000 m	3

	2000-4000 m	4
	>4000 m	5
Slope	0-5 (%)	5
	5-10 (%)	4
	10-15 (%)	3
	15-20 (%)	2
	>20 (%)	1
Industrial Area	<1000 m	5
	1000-2000 m	4
	2000-4000 m	3
	4000-6000 m	2
	>6000 m	1

- **Calculation of the Weights of Each Criterion**

To calculate the weight of each criterion, perform the following steps:

1. Calculate the Eigenvector of the Comparison Matrix: Solve the following equation:

$$C \cdot W = \lambda_{max} \cdot W \qquad \text{Eq. 5}$$

where:

- W is the vector of criteria weights (which we need to determine),
- λ_{max} is the principal eigenvalue of the matrix (which indicates the consistency of the pairwise comparisons).

2. Normalise the Eigenvector: Normalise the vector W by dividing each entry by the sum of all entries:

$$W_i = \frac{w_i}{\sum_{i=1}^{n} w_i} \qquad \text{Eq. 6}$$

where W_i is the normalised weight for criterion i.

3. Consistency Check: The Consistency Ratio (CR) checks how consistent the pairwise comparisons are. If the CR exceeds 0.1, the comparisons should be revised.

$$CR = \frac{CI}{RI} \qquad \text{Eq. 7}$$

where:

- CI (Consistency Index) is calculated as: $CI = \frac{\lambda_{max}-n}{n-1}$
- RI (Random Index) is a value that depends on the size of the matrix. For an (n x n) matrix, the typical values of RI are found in a predefined table.
- If CR > 0.1, you should revise the pairwise comparisons.

4. Pairwise Comparisons for Each Land Parcel

Next, perform pairwise comparisons for each land parcel (site). For each site and criterion, compare how suitable the site is in terms of the selected criterion. For example, if you're comparing two sites based on soil quality, evaluate how well each site supports the desired soil type.

Construct a comparison matrix for each site:

$$C = \begin{bmatrix} 1 & a_{12}^{site} & a_{13}^{site} & \dots & a_{1n}^{site} \\ 1/a_{12}^{site} & 1 & a_{23}^{site} & \dots & a_{2n}^{site} \\ \vdots & \vdots & 1 & \vdots & \vdots \\ \vdots & \vdots & \vdots & 1 & \vdots \\ 1/a_{1n}^{site} & 1/a_{2n}^{site} & 1/a_{3n}^{site} & \dots & 1 \end{bmatrix}$$

Calculate the Land Suitability Score

For each site, multiply the normalised weights of the criteria by the values in the comparison matrix. The final score for each site is the weighted sum of the scores for all criteria.

where:

$S_{site} = \sum_{i=1}^{n} w_i \cdot a_{ij}^{site}$ Eq. 8

S_{site} is the suitability score for a particular site,

w_i is the weight of criterion i,

a_{ij}^{site} is the relative importance of site j under criterion i.

Rank the Sites

After calculating the suitability scores for all sites, rank them from the most suitable to the least suitable. The site with the highest score is the most suitable for the proposed activity.

$Ranked\ Sites = \{S_{site\ 1}, S_{site\ 2}, S_{site\ 3}, \dots\dots\dots, S_{site\ n}\}$

The site with the highest score is the most suitable for the land use.

Using the AHP methodology in land suitability analysis allows for a systematic and consistent approach to evaluate and prioritize land parcels based on multiple criteria. By using pairwise comparisons, eigenvalue calculations, and a final suitability score, this methodology helps decision-makers identify the most appropriate land for their intended purpose, considering both

quantitative and qualitative factors. Check the consistency ratio (CR) to ensure valid comparisons (CR < 0.1 acceptable). Weights are integrated into the GIS model for weighted overlay.

4.3. GIS-Based Weighted Overlay Analysis

Reclassify all raster layers (criteria) into standardised suitability scales (e.g., 1–5). Apply the AHP-derived weights to each layer using the Raster Calculator tool. Generate a final suitability map showing areas classified as: Highly Suitable, Suitable, Moderately Suitable, Low Suitable, and Not Unsuitable, overlay constraint layers (e.g., protected zones, water bodies) to mask out restricted areas(*How Weighted Overlay Works—ArcGIS Pro | Documentation*).

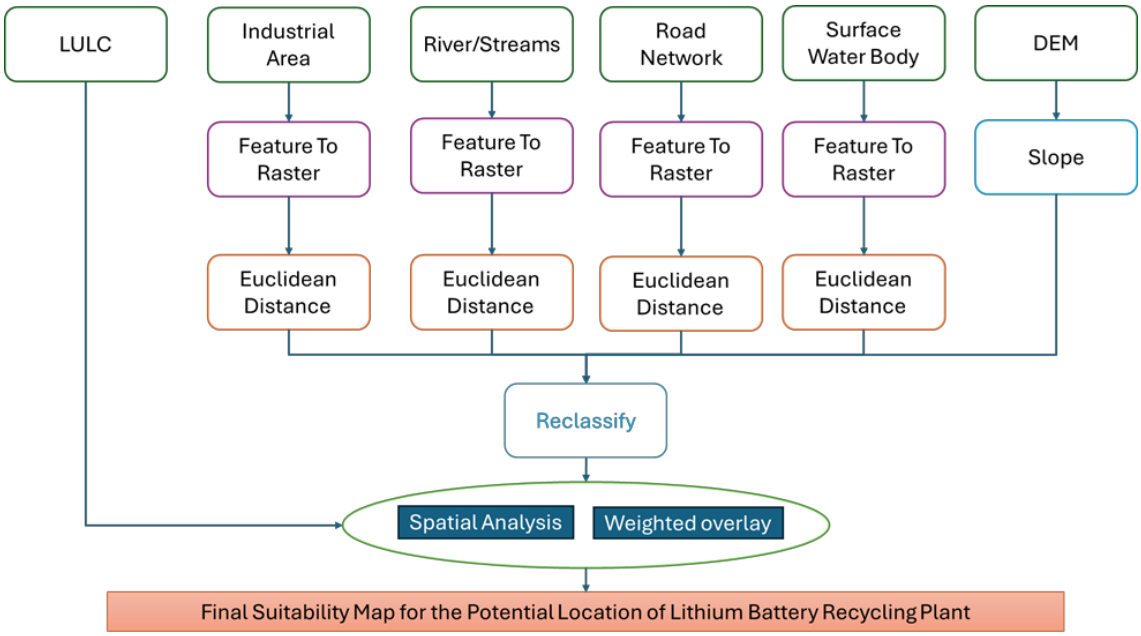

Figure 8: AHP integrated suitability analysis methodology

4.4. Validation

Final site options are shortlisted from highly suitable zones. Cross-verification is done using ground data, regulatory constraints, and logistic feasibility. Recommendations are supported with a multi-criteria ranking table comparing top locations. Awareness has been brought regarding this requirement of planned battery recycling facilities, a regulation framework, and sustainable solutions for handling waste in countries that are moving toward addressing the environmental challenges that EV adoption has created.

Chapter 5

5. Results and Discussion

5.1. Outlier Detection

The result of the Z score is given in Figure 3. It serves as a valuable tool for anomalies. It's worth noting that, in this time series data, the z-score statistical test did not reveal anomalies.

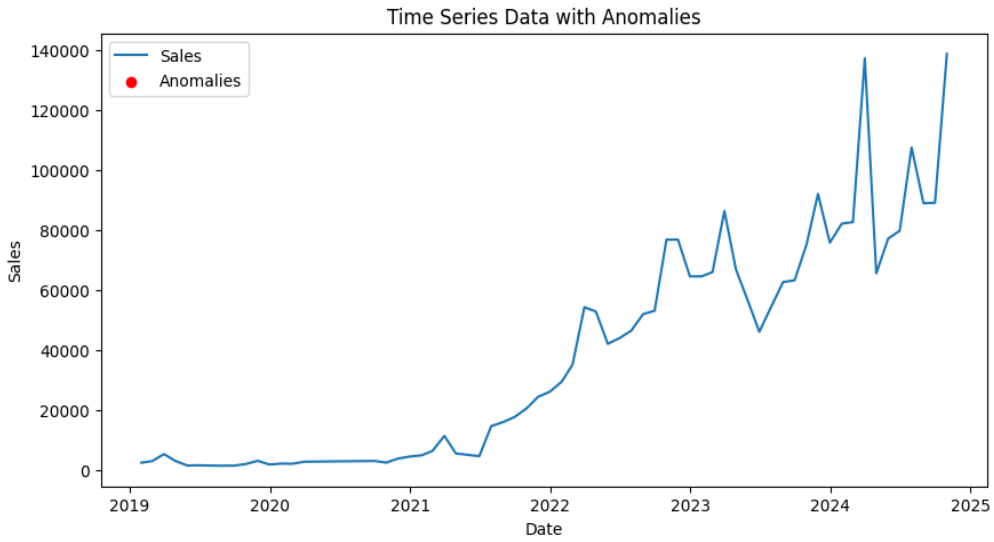

Figure 9: Data plot with anomalies

5.2. Seasonality and trend:

1. Trend

Upward Trend:

There is a clear exponential increase in sales starting around mid-2021, with steep growth afterwards. Early Flat Period. From 2016 to mid-2020, the sales remained low and flat, suggesting minimal market penetration or adoption in the early years.

2. Seasonality

There appears to be repeating peaks and dips in the recent years (2022–2025), especially in the last quarters of each year. This suggests potential seasonal behaviour, likely influenced by Government incentives or policy rollouts. Festive buying seasons (e.g., Diwali in India), End-of-year inventory clearance.

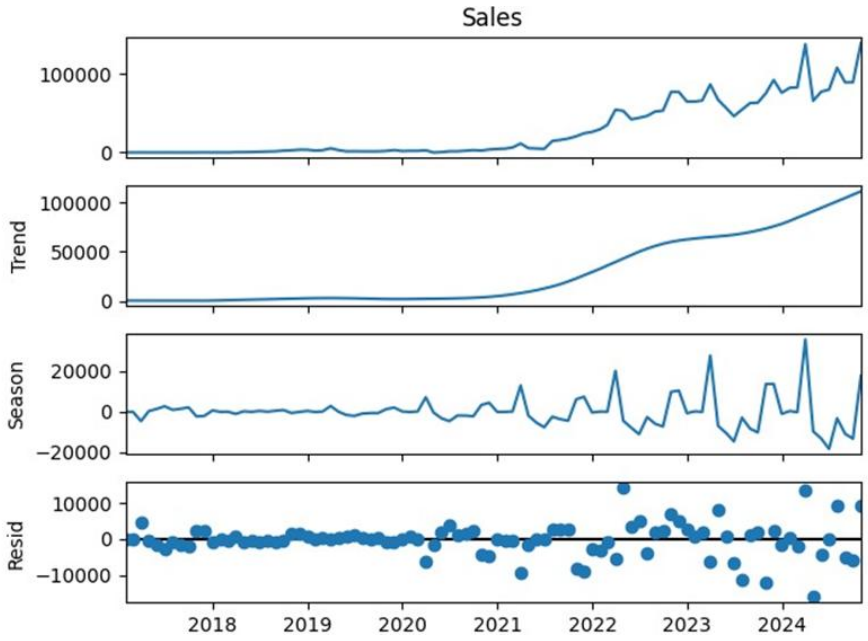

Figure 10: Seasonality and trend analysis plots

5.3. Stationarity check and differencing

Sales data from EVs is subjected to an Augmented Dickey-Fuller (ADF) test to check the stationarity. The EV sales data used in this study represent a non-stationary monthly time series. The result shows that the original time series data was non-stationary with test statistics 1.218 and a p-value of 0.95, which is higher than all critical values at the 1%, 5%, and 10% levels. After applying second differencing, the series remains non-stationary, with a p-value of 0.5877, still higher than 0.05 still exceeding the threshold for rejecting null hypothesis of a unit root however after second differencing, the test statistics sharply decreased to -6.873 with a highly p-value of 0.0000001 well below all critical values (1%: -3.551; 5%: -2.914; 10%: -2.955). This confirms that the time series became **stationary after second differencing**, justifying the use of **d=2** in the SARIMA model configuration. In achieving stationarity, all the test statistics are presented in the table, No.2. The second differencing gives a mean and a stable variance. it is adopted for further study.

Table 7: Stationarity statistics

Differencing Level	Test Statistic	p-value	Critical Value (1%)	Critical Value (5%)	Critical Value (10%)	Stationarity Conclusion

Original Data	1.218	0.996	-3.544	-2.91	-2.593	**Non-stationary**
After First Differencing	-1.388	.5877	-3.551	-2.914	-2.595	**Non-stationary**
After Second Differencing	-6.873	0.0000001	-3.551	-2.914	-2.955	**Stationary**

5.4.Model Identification and Parameter Estimation

5.4.1. Model Identification Using ACF and PACF:

After performing second differencing, the data were found to be stationary. The test statistics are presented in Table 2, indicating that the d value is 2 for second-order differencing. The ACF and PACF plots help to determine the parameters for the SARIMA model. In the ACF plot, Figure 5, significant lags were observed up to approximately lag 30. This suggests the presence of a moving average (MA) process, at lag 1, 3, and 4, showed a clear spike beyond the 95% confidence bound, which signifies a strong correlation at these lags, indicating the order q could be 1,3 and 4. The PACF plot, Figure 6, shows clear spikes at lags 1 and 3, followed by a sharp cutoff, suggesting an autoregressive (AR) process with order p values 1 and 3.

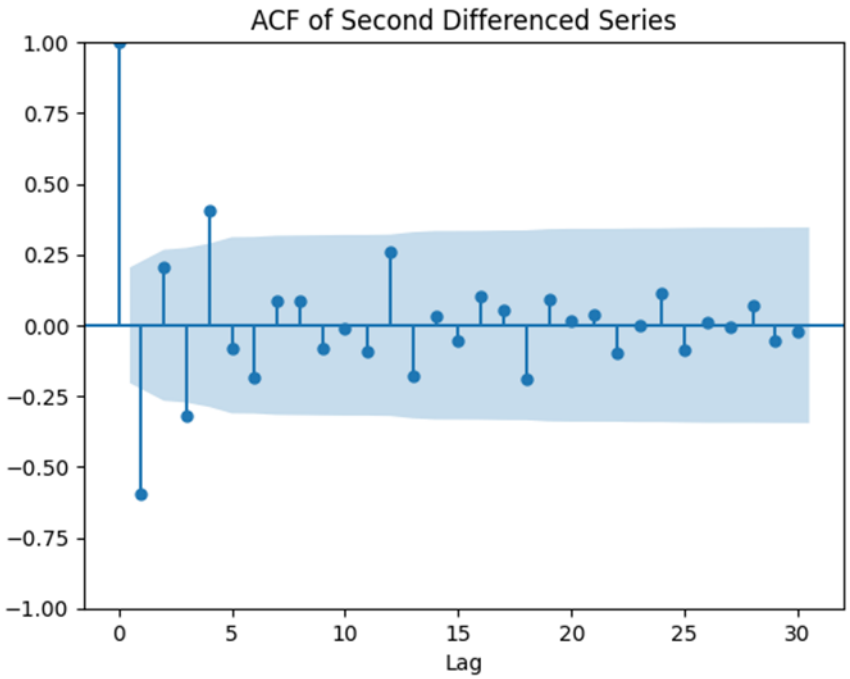

Figure 11: ACF Plot of the Second time differenced of the original sales data

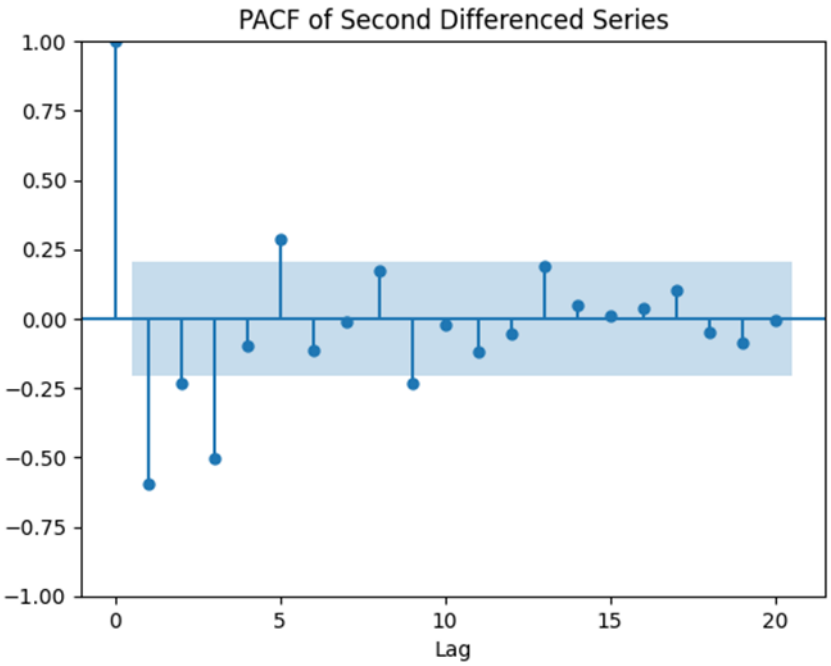

Figure 12: PACF plot of the second time differenced of the original sales data

In order to identify the seasonal parameters, the annual seasonality exhibited by the monthly E2Ws sales series, season differencing at the shift of the time series of 12 months of the original series was performed. The Autocorrelation Function (ACF) of the differenced series showed sharp spikes at lags 1 and 4, thereafter declining gradually. It is a sign of a strong seasonal moving average (MA) component. So, from the ACF of the seasonal component, we can take the moving average parameter Q, which can be taken in between 1 and 4 to build the SARIMA model. At the same time, the Partial Autocorrelation Function (PACF) plot of the seasonal component showed significant spikes at lags 1 and 2 beyond the 95% confidence interval. At these lags, good autocorrelation in the PACF plot Figure 6 after lag 2 became fainter. So, to build the SARIMA model, we can start with the seasonal Autoregressive parameters 1 and 2. To empirically evaluate this, multiple SARIMA models were tested with varying values of non-seasonal moving average parameter q, autoregression parameter p. and Seasonal MA Parameter Q, seasonal AR parameter P. The non-seasonal parameter (3, 2, 3) and seasonal parameter (2, 1, 3, 12) demonstrated superior performance across key forecasting metrics, including a lower MAPE, MAE and a reasonably high score R^2, in these observations, which are consistent with identifying SARIMA parameters for a dataset showing trends and seasonality.

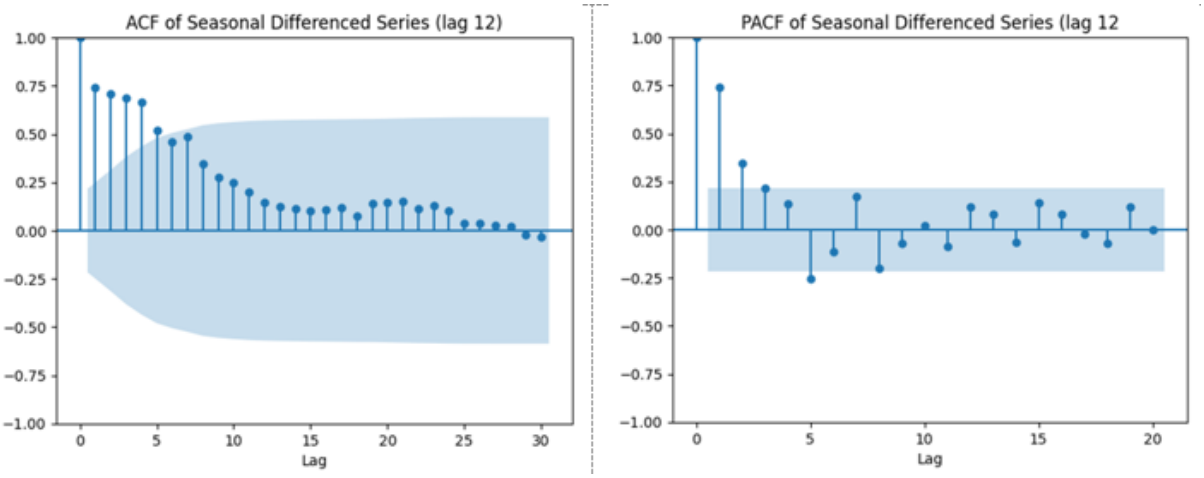

Figure 13: ACF and PACF plot of the seasonal component of the time series data

5.4.2. Model Parameter Estimation and Fitting:

Based on the analysis of the seasonal and non-seasonal ACF and PACF plots, a range of SARIMA model specifications was evaluated. The best-fitting model was identified through iterative testing using model selection criteria: Akaike Information Criterion (AIC), Bayesian Information Criterion (BIC), and Hannan-Quinn Information Criterion (HQIC). The SARIMA (3,2,3) (2,1,3) [12] model demonstrated optimal performance with the lowest values across all criteria: AIC = 873.094, BIC = 893.360, and HQIC = 880.422. The model also achieved a log-likelihood of –424.547, indicating a good balance between model fit and complexity.

Table 8 summarises the key statistics: This model effectively captures both the non-seasonal and annual seasonal dynamics in the monthly sales time series data from January 2017 to October 2024 (n = 94 observations).

Table 8: Evaluation matrices

Matrices	Value
Log-Likelihood	-424.547
AIC	873.094
BIC	893.360
HQIC	880.422

5.5. Model Validation: Training and Testing

To evaluate the predictive performance of the selected SARIMAX (3,2,3) (2,1,3,12) model, the dataset comprising 94 monthly observations from January 2017 to October 2024 was

partitioned into training and testing sets. The first 77 observations (January 2017 to May 2023) were used to train the model, while the remaining observations (August 2023 to October 2024) were reserved for testing and validation purposes.

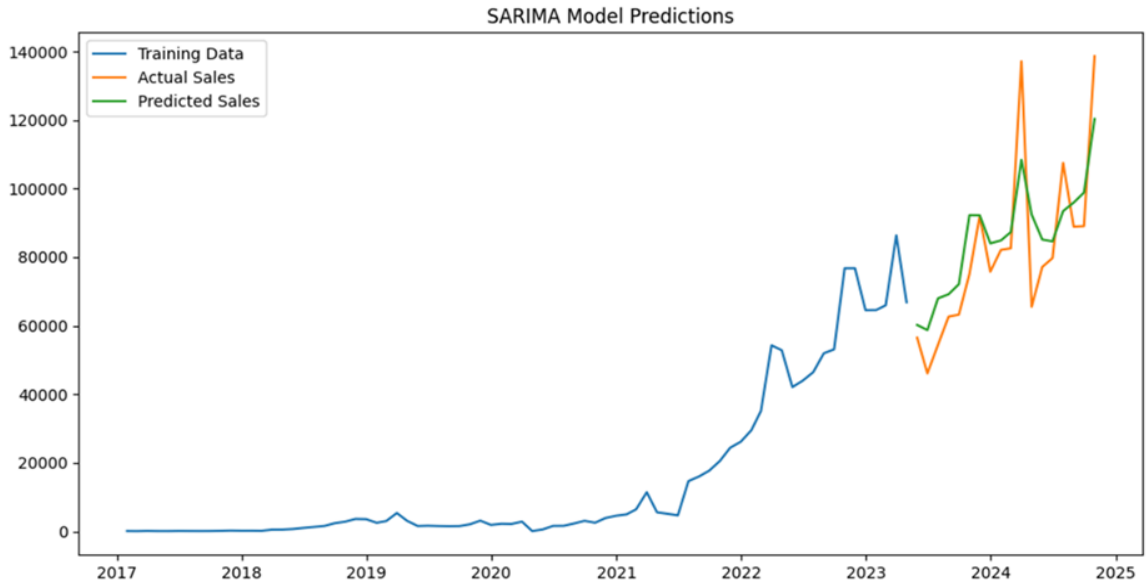

Figure 14: Plot of the fitted SARIMA model over training and testing

The model was trained on the training dataset using the maximum likelihood estimation approach. After fitting, one-step-ahead dynamic forecasts were generated for the test set, and the forecasted values were compared with the actual sales data to assess predictive accuracy. The model's performance was evaluated using standard statistical metrics, including Mean Absolute Percentage Error (MAPE), Root Mean Squared Error (RMSE), Mean Absolute Error (MAE), and the coefficient of determination (R^2).

The results yielded a MAPE of 10.93%, indicating a relatively low average percentage deviation between predicted and actual values. The RMSE was 13897.8, and the MAE was 9499.81, suggesting a reasonable error magnitude. Furthermore, the model achieved an R^2 score of 0.678, which confirms that a substantial proportion of the variance in E2Ws sales is explained by the fitted model. These metrics demonstrate that the SARIMAX model offers robust forecasting capability and generalises well to unseen data. The validated model was then used for full-sample forecasting and diagnostic analysis.

Table 9: Standard statistical matrix

Parameter	Values
MAPE	10.93%
R^2	0.678
MAE	9499.81
RMSE	13897.8

5.6. Evaluation matrices

Reasonable Accuracy (MAPE 10.93%): With a Mean Absolute Percentage Error of 10.93%, the model achieves a commendable level of accuracy, indicating that it reliably captures trends and seasonality in the data, which can be used to make long-term forecasts.

Explained Variance (R^2 0.678): The R^2 value of 0.678 shows that the model explains a significant 0.678% of the variance in the data, providing valuable insights into the underlying patterns and trends.

Trend and Seasonality Capture: The model successfully identifies and predicts the increasing trend in battery waste over time, making it a reliable tool for long-term planning and infrastructure development.

The model demonstrates strong predictive capabilities with reliable accuracy and practical trend analysis. These results underscore its utility in supporting sustainable waste management strategies and decision-making for the growing two-wheeler EV market.

The model's robustness was assessed using a 77-month training and 17-month testing, which is approximately an 80-20 split, ensuring validation of unseen data. Although SARIMA provided valuable insights into the time series patterns, the exponential sales growth hints at the potential for improvement by integrating models designed for rapid trend escalation. Further, this SARIMA model is fitted and used for forecasting the monthly sales till 2030. Based on this forecast, further, the potential battery waste is calculated till 2030

5.7. Model Diagnostics

The diagnostic evaluation of the fitted SARIMA (3,2,3) (2,1,3) [12] model demonstrates that the residuals generally satisfy the assumptions of randomness and normality. The Ljung–Box Q-test at lag 1 yields a test statistic of 0.74 ($p = 0.39$), indicating no significant autocorrelation and suggesting that the residuals behave like white noise. The Jarque–Bera test confirms the normality of residuals (JB = 0.30, $p = 0.86$), with a skewness of –0.20 and kurtosis of 2.83,

indicating a nearly symmetric distribution. As illustrated in Figure 15, the standardised residuals oscillate randomly around zero without discernible patterns, while the histogram and kernel density estimate closely approximate a normal distribution. The normal Q–Q plot shows that most residuals lie along the 45-degree line, with only slight deviations at the tails, reinforcing the normality assumption. Furthermore, the correlogram of residuals shows all autocorrelation values within the 95% confidence interval, reaffirming the absence of residual autocorrelation. However, the model reveals some evidence of heteroskedasticity (H = 4.13, p = 0.02), suggesting that the variance of the residuals may vary over time. Although this does not critically impair the model's predictive accuracy, it may influence the width and reliability of forecast intervals. Overall, the residual diagnostics (Figure 15) support the adequacy of the SARIMA model in capturing the underlying structure of the time series data for reliable forecasting.

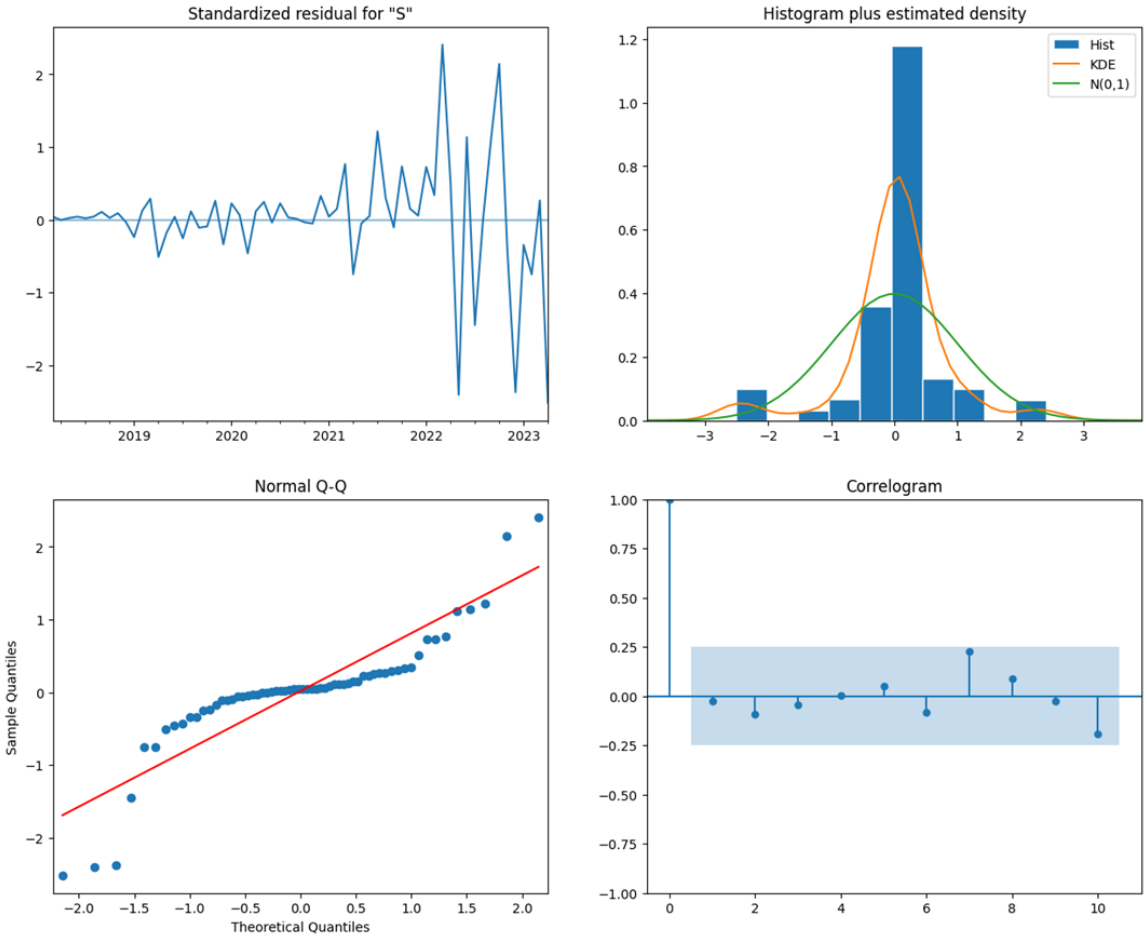

Figure 15: Model diagnostic plot

5.8. Forecasting future sales using the optimised SARIMA model:

After successfully finalising the SARIMA model, which demonstrated satisfactory accuracy in its predictions, we will leverage this model to project future sales figures from November 2024 through December 2030. This forecasting will provide valuable insights into expected sales trends over the coming years. Notably, the forecast indicates a significant increase in sales of E2Ws vehicles, demonstrating an upward trend throughout the forecast period. The projected monthly sales figures increase from approximately 120,747 units in November 2024 to 341,345 units by December 2030, representing nearly a tripling of monthly demand over the forecast horizon. These upward trends reflect the anticipated expansion of the India EV market, driven by policy incentives, cost reduction and rising Environmental awareness. Table 12, showing the monthly E2Ws Sales forecasts from the SARIMA model, is provided, along with another table displaying the annual sales forecasts over six years, highlighting projected trends and expected growth. To further illustrate the data, the monthly sales forecasts produced by the model are visually represented in Figures 10 and 11.

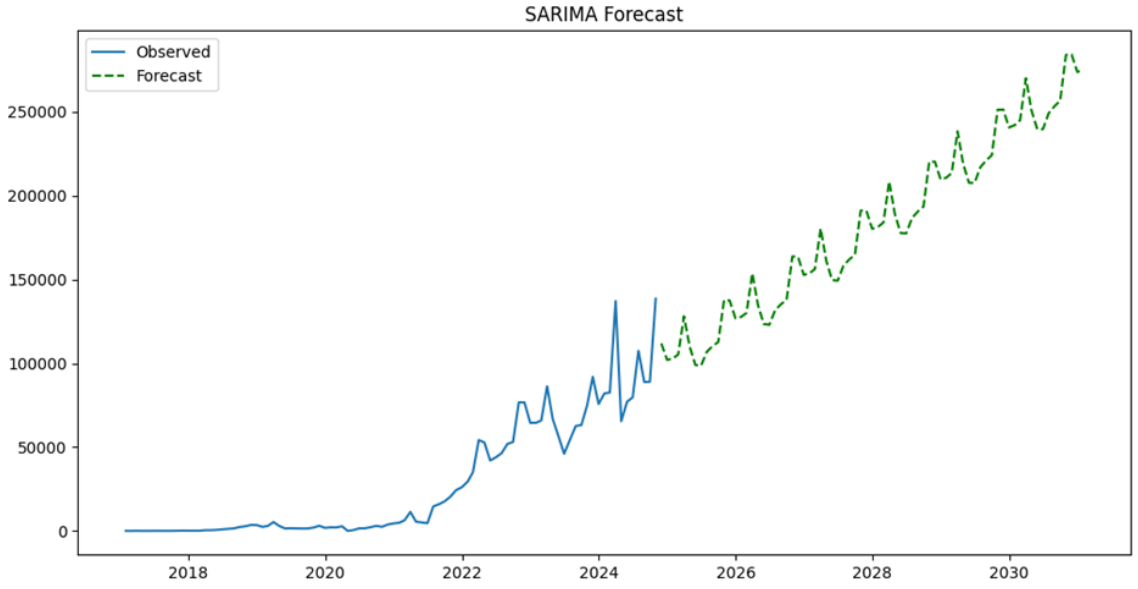

Figure 16: SARIMA model forecasted and past data plot

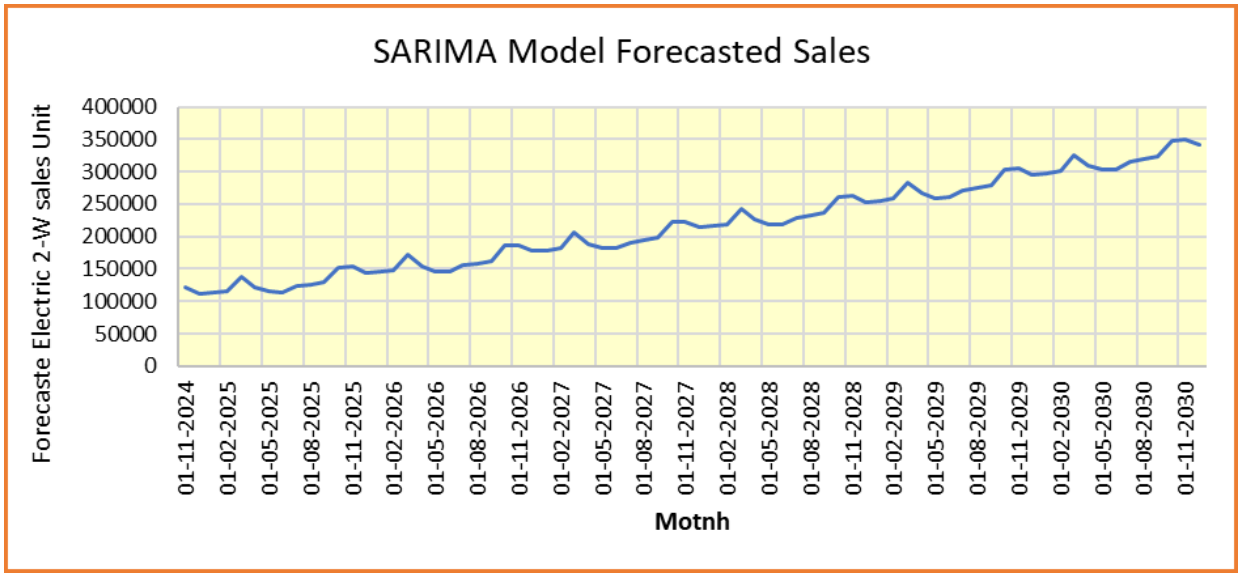

Figure 17: Forecasted monthly sales till 2030

5.9. Estimation of Potential EV Waste

The forecasted E2Ws sales data were further utilised to estimate the potential LIB waste that will accumulate as a result of increased adoption. This estimation was grounded in a base case scenario where the average specific energy of battery cells was assumed to be 210 Wh/kg, derived as the mean of the representative range (160 Wh/kg to 260 Wh/kg) commonly observed in lithium iron phosphate (LFP) and nickel manganese cobalt (NMC) chemistries. Furthermore, the average battery capacity per E2Ws was set at 2.025 kWh, as referenced from industry-based benchmarks and reports such as the ICCT Working Paper (Gode et al., 2021).

By combining these parameters, the estimated battery mass per unit was calculated and applied to the SARIMA-forecasted sales figures to compute monthly and annual projections of LIB waste. The waste estimation considers only the cell mass of the battery, which is directly linked to material recovery and recycling system design.

The results indicate a substantial and accelerating increase in battery waste. In 2025, the total estimated potential battery waste corresponding to forecasted E2Ws Sales is approximately 17.17 million kilograms, which nearly doubles to 37.02 million kilograms by 2030. Monthly projections reveal a consistent upward trend, with peaks in months exhibiting strong sales, such as March and October. This exponential growth reflects the cumulative impact of widespread E2Ws adoption and aligns with the battery replacement cycles reaching end-of-life.

Figure 18 offers insights into the Estimated Potential Future LIB waste corresponding to forecasted E2Ws, providing a clear graphical overview of the anticipated sales patterns over

time. Along with the monthly potential battery waste from E2Ws Sales, the annual potential waste is also calculated from the monthly Sales Data for both historical sales and Forecasted Sales The results are visualized in Figure 19 and Figure 20, while Table 10 presents the potential battery waste corresponding E2Ws from past sales data and table 11 illustrates future potential waste from forecasted data

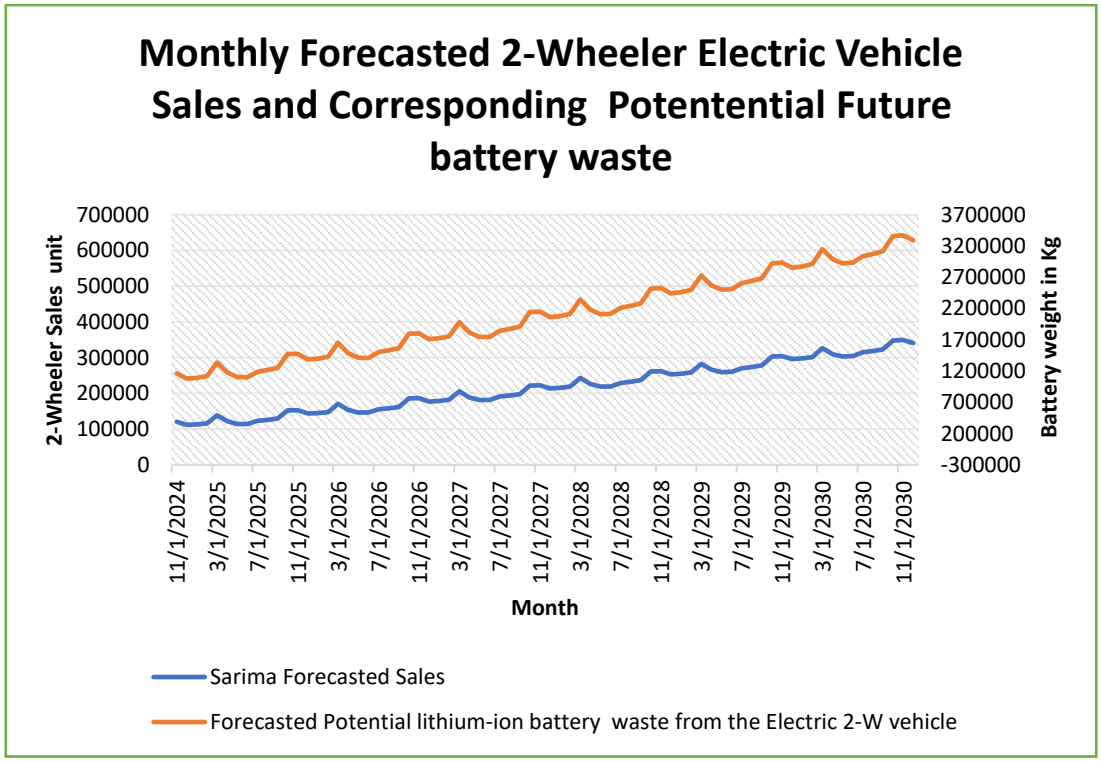

Figure 18: Monthly forecasted sales and corresponding battery mass waste potential

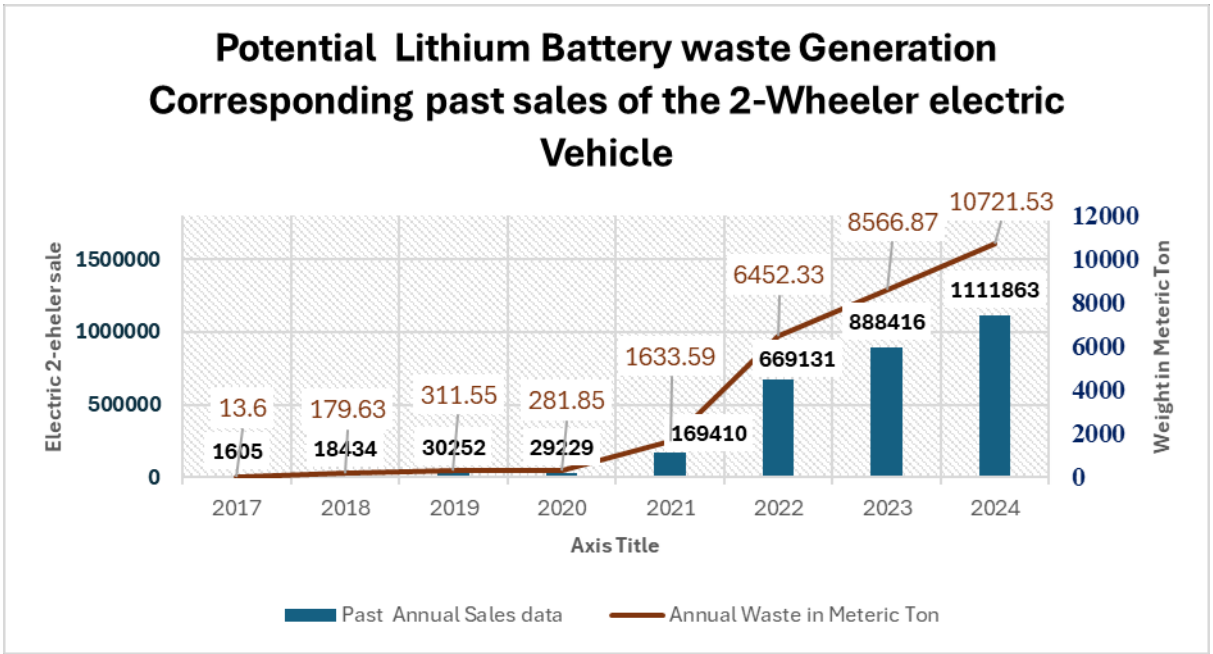

Figure 19: Projected LIB waste generation from past sales data

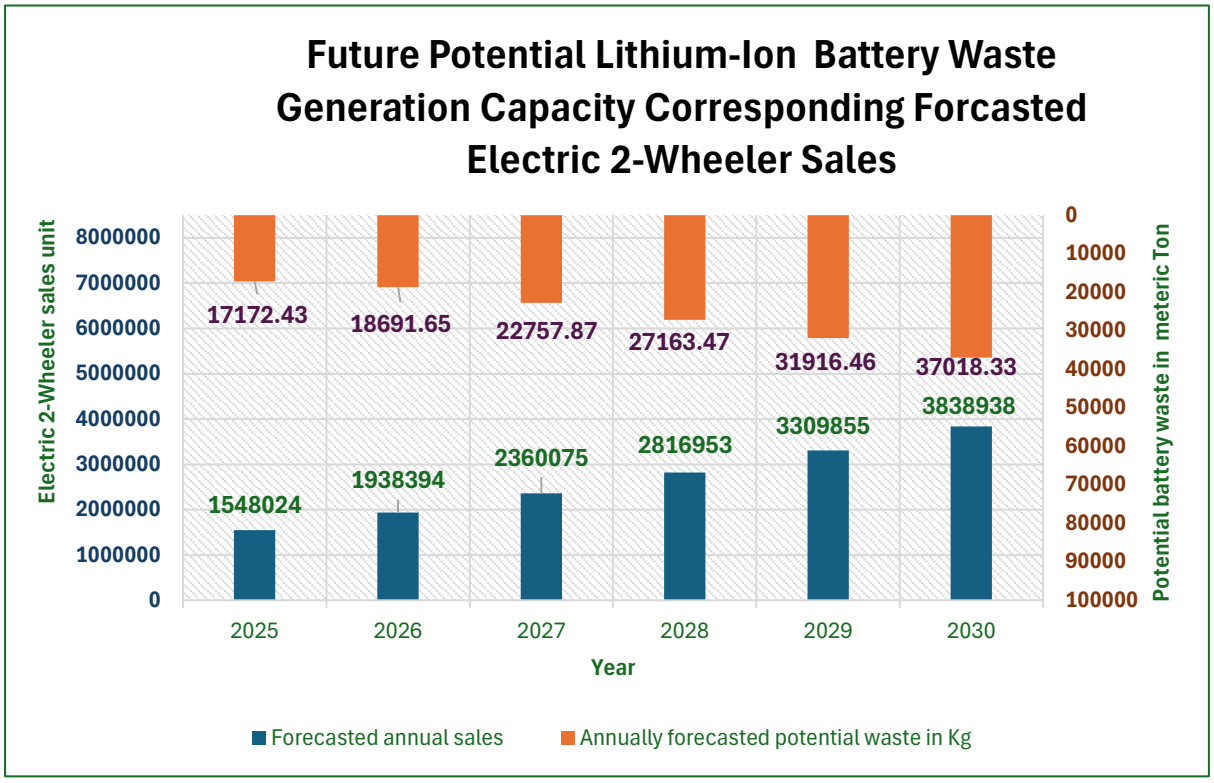

Figure 20: Forecasted sales and corresponding potential LIB waste

Table 10: Estimated annual waste in Kg from past sales

Year	2017	2018	2019	2020	2021	2022	2023	2024
Annual Waste in Kg	13596.43	179636.8	311551	281851	1633596	6452335	8566869	10721536

Table 11: Estimated projected annual waste from forecasted EV Sales

Year	2025	2026	2027	2028	2029	2030
Annually forecasted potential waste in Kg	17172434	18691656	22757866	27163475	31916459	37018331

Table 12: Estimated future EVs waste from forecasted Two-Wheeler sales

Month	Sarima Forecasted Sales	Estimated Potential Future EVswaste from Forecasted Electric Two-Wheler Vehicle in Kg	Month	Sarima Forecasted Sales3	Estimated Potential Future EVswaste from Forecasted Electric Two-Wheler Vehicle in Kg
30-11-2024	120747	1164346.1	31-01-2028	215665	2079626.8
31-12-2024	112074	1080713.6	29-02-2028	219028	2112055.7
31-01-2025	113262	1092169.3	31-03-2028	242957	2342799.6
28-02-2025	116139	1119911.8	30-04-2028	225925	2178562.5
31-03-2025	138648	1336962.9	31-05-2028	218938	2111187.9
30-04-2025	122350	1179803.6	30-06-2028	219090	2112653.6
31-05-2025	114661	1105659.6	31-07-2028	229277	2210885.4
30-06-2025	114305	1102226.8	31-08-2028	232621	2243131.1
31-07-2025	123386	1189793.6	30-09-2028	236692	2282387.1
31-08-2025	126228	1217198.6	31-10-2028	261163	2518357.5
30-09-2025	129433	1248103.9	30-11-2028	262182	2528183.6
31-10-2025	152702	1472483.6	31-12-2028	253415	2443644.6
30-11-2025	153124	1476552.9	31-01-2029	255362	2462419.3
31-12-2025	143786	1386507.9	28-02-2029	258975	2497258.9
31-01-2026	145045	1398648.2	31-03-2029	283159	2730461.8
28-02-2026	147973	1426882.5	30-04-2029	266370	2568567.9
31-03-2026	171250	1651339.3	31-05-2029	259633	2503603.9

30-04-2026	154032	1485308.6	30-06-2029	260036	2507490
31-05-2026	146547	1413131.8	31-07-2029	270477	2608171.1
30-06-2026	146244	1410210	31-08-2029	274070	2642817.9
31-07-2026	155859	1502926.1	30-09-2029	278394	2684513.6
31-08-2026	158750	1530803.6	31-10-2029	303119	2922933.2
30-09-2026	162296	1564997.1	30-11-2029	304388	2935170
31-10-2026	186181	1795316.8	31-12-2029	295872	2853051.4
30-11-2026	186727	1800581.8	31-01-2030	298070	2874246.4
31-12-2026	177490	1711510.7	28-02-2030	301934	2911506.4
31-01-2027	178947	1725560.4	31-03-2030	326371	3147148.9
28-02-2027	182070	1755675	30-04-2030	309831	2987656.1
31-03-2027	205723	1983757.5	31-05-2030	303346	2925122.1
30-04-2027	188491	1817591.8	30-06-2030	304000	2931428.6
31-05-2027	181253	1747796.8	31-07-2030	314692	3034530
30-06-2027	181161	1746909.6	31-08-2030	318537	3071606.8
31-07-2027	191086	1842615	30-09-2030	323112	3115722.9
31-08-2027	194186	1872507.9	31-10-2030	348090	3356582.1
30-09-2027	198002	1909305	30-11-2030	349610	3371239.3
31-10-2027	222209	2142729.6	31-12-2030	341345	3291541.1
30-11-2027	222980	2150164.3			
31-12-2027	213967	2063253.2			

5.10. Scenario-Based Analysis of Battery Lifespan and Waste Contribution

To enhance the robustness of battery waste estimation, this study incorporated realistic battery degradation patterns by modelling three different lifespan scenarios. As lithium-ion batteries typically retire once their usable capacity drops below 80% of the original, the effective EOL contribution was recalculated under three lifespan assumptions: a low-performing scenario (4 years), a base-case scenario (6 years), and an optimistic scenario (8 years). For each scenario, the projected battery waste from E2Ws sales was shifted forward in time to reflect the actual year when the battery is likely to reach its end of service.

This scenario-based temporal adjustment resulted in significantly different annual waste contributions over the forecast horizon. For instance, under the 4-year scenario, waste volumes rise earlier, peaking sooner due to quicker battery turnover. In contrast, the 8-year scenario delays peak waste generation, extending the material load into the 2030s. The base case (6 years) provides a balanced estimate aligned with industry standards. Figure 20 presents a comparative visualisation of annual battery waste contributions across the three scenarios, offering a dynamic and forward-looking view of waste emergence patterns. These insights are

critical for aligning infrastructure deployment, recycling capacity planning, and policy implementation with actual battery retirement timelines.

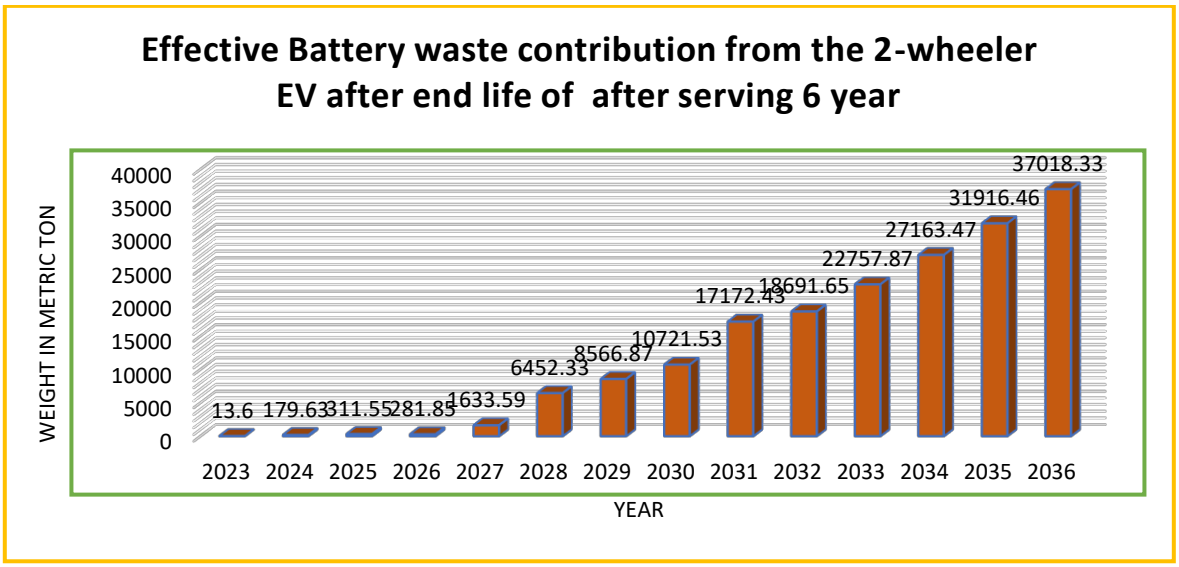

Figure 21: Effective battery waste contribution in the base case scenario of a 6-year battery life span

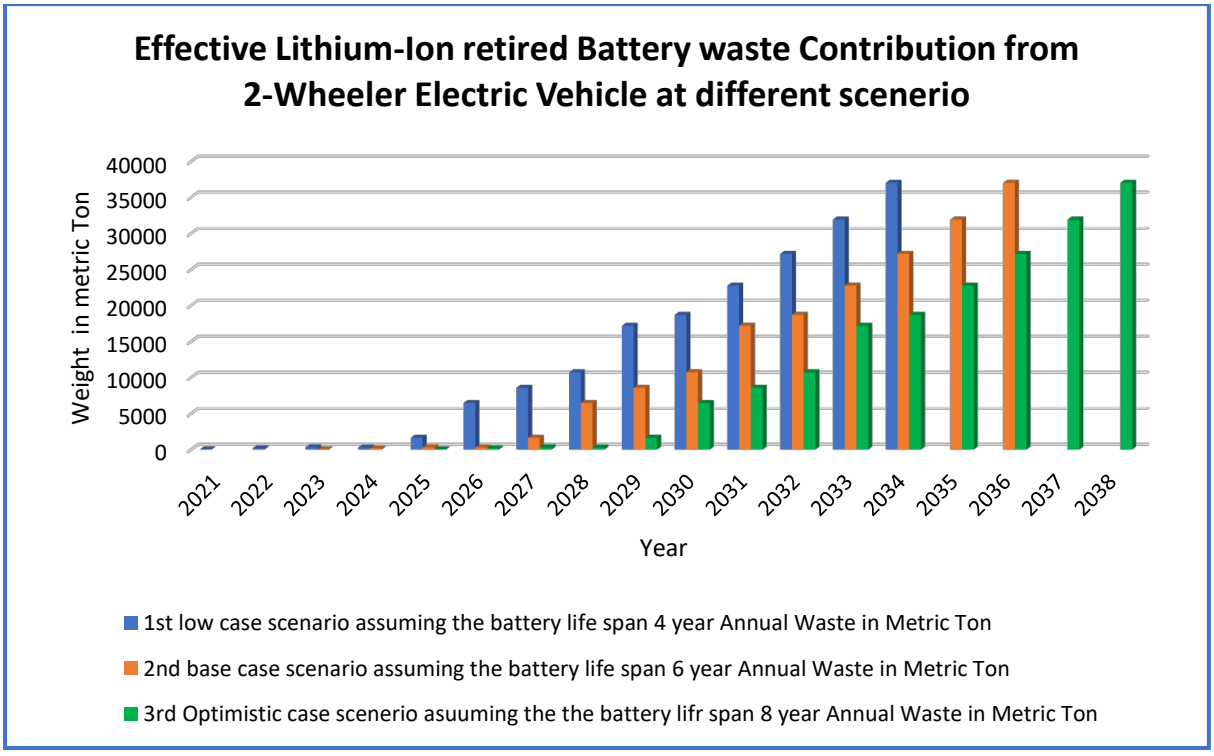

Figure 22: Waste contribution after the end of life of lithium-ion batteries in all three scenarios

5.11. Site Suitability Result

This section presents the reclassification results of each spatial criterion used in the site suitability analysis. The reclassified raster layers represent the spatial distribution of suitability classes on a scale of 1 (least suitable) to 5 (most suitable)(Akther et al., 2019). These individual suitability layers form the basis for the multi-criteria decision-making process using the AHP model.

5.11.1. Slope

The slope map was derived from the SRTM DEM and reclassified into five suitability classes. Areas with a slope of **0–5%**, which are ideal for construction and industrial infrastructure, were assigned the highest suitability score (5). These flat terrains are mostly concentrated in the central and northern parts of the Indore district. Conversely, areas with slopes greater than **20%** were considered unsuitable (score 1) due to difficulties in construction and drainage. Overall, the majority of the study area exhibited gentle to moderate slopes, making it favourable for industrial development.

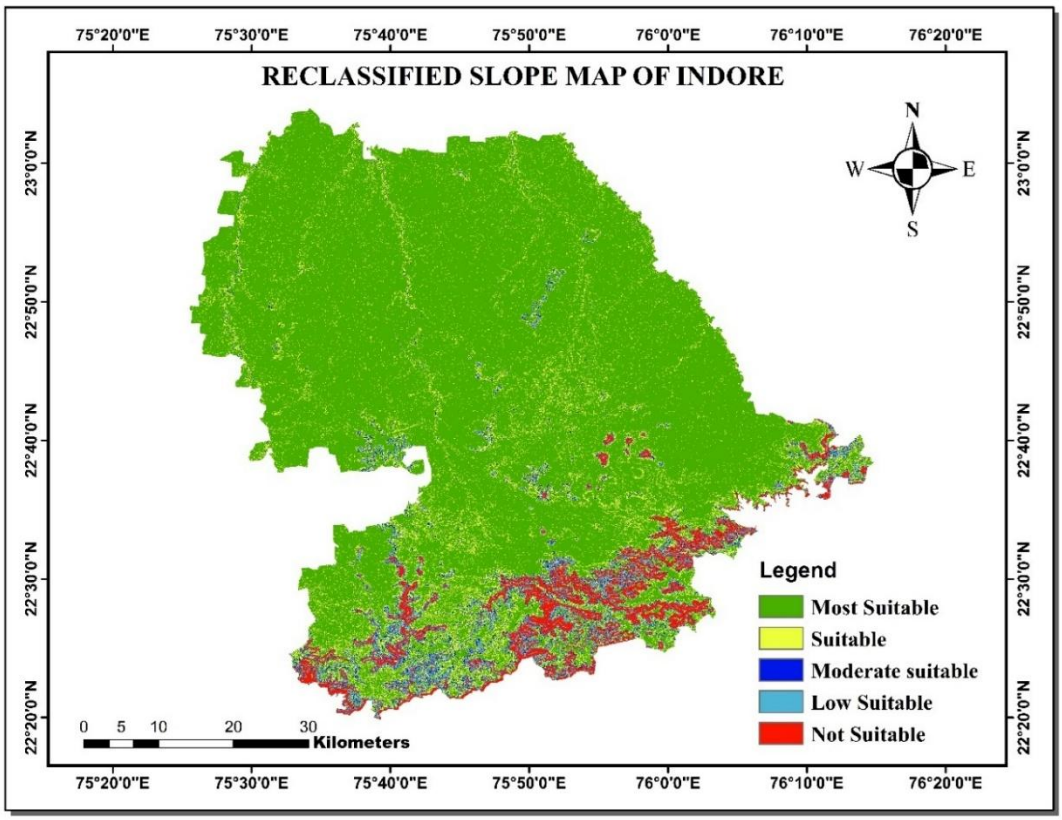

Figure 23: Reclassified slope map of Indore district

5.11.2. Proximity to Major Roads

The road network layer was extracted from OpenStreetMap and analysed based on proximity to major roads. The analysis revealed that areas within 250–750 meters from major roads received the highest suitability score (5), as they offer ease of transportation without being too close to cause environmental and safety concerns. Areas within <250 meters were assigned a low score (1) due to possible restrictions and safety issues related to proximity to road corridors. Most of the central and eastern parts of Indore showed high suitability in terms of road accessibility.

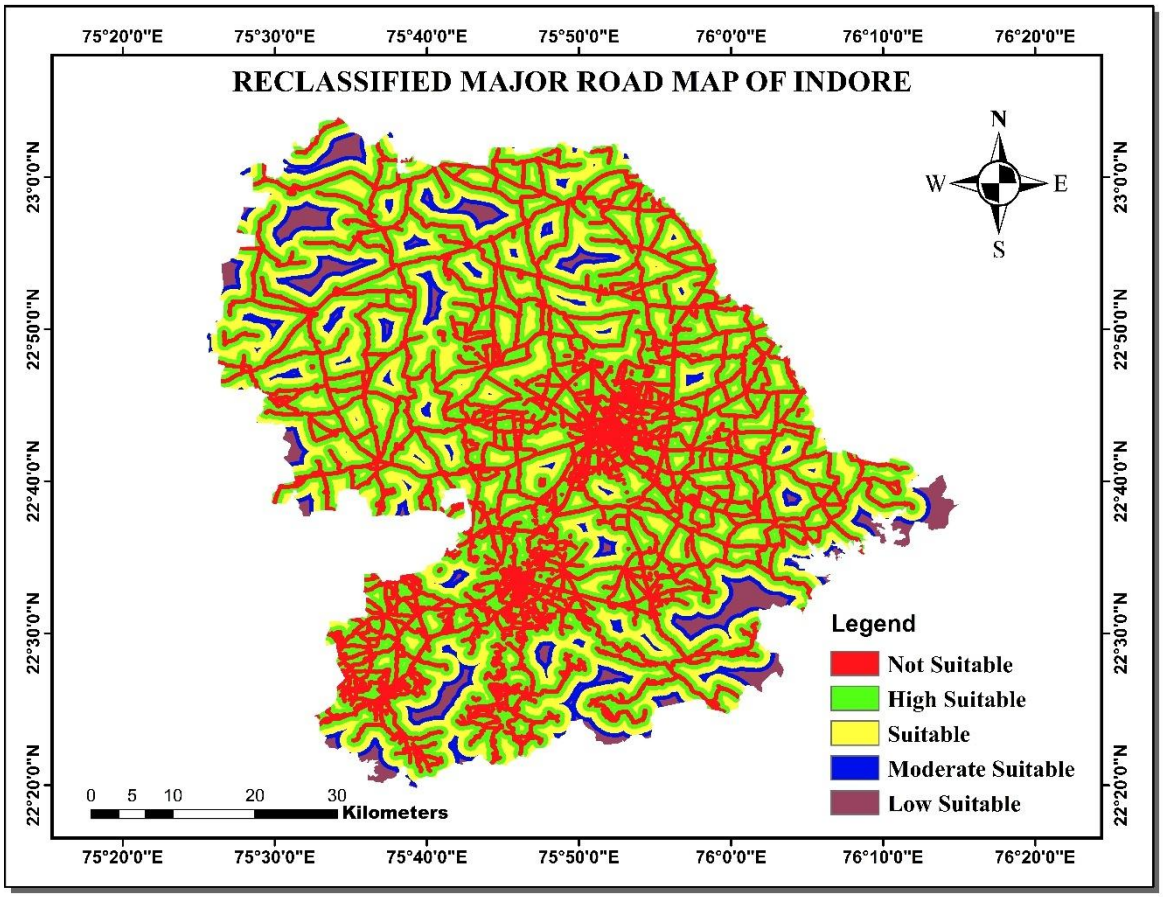

Figure 24: Reclassified Road map of Indore district

5.11.3 Proximity to Surface Water Bodies

Surface water bodies were also mapped from OpenStreetMap data. Locations farther than 4000 meters from water bodies were considered the most suitable, with a score of 5 to avoid potential contamination risks. Areas closer than 250 meters were given the lowest suitability score of 1.

The reclassified map showed that the north-western and some central zones of Indore district were far from surface water bodies and thus highly suitable for setting up a recycling plant.

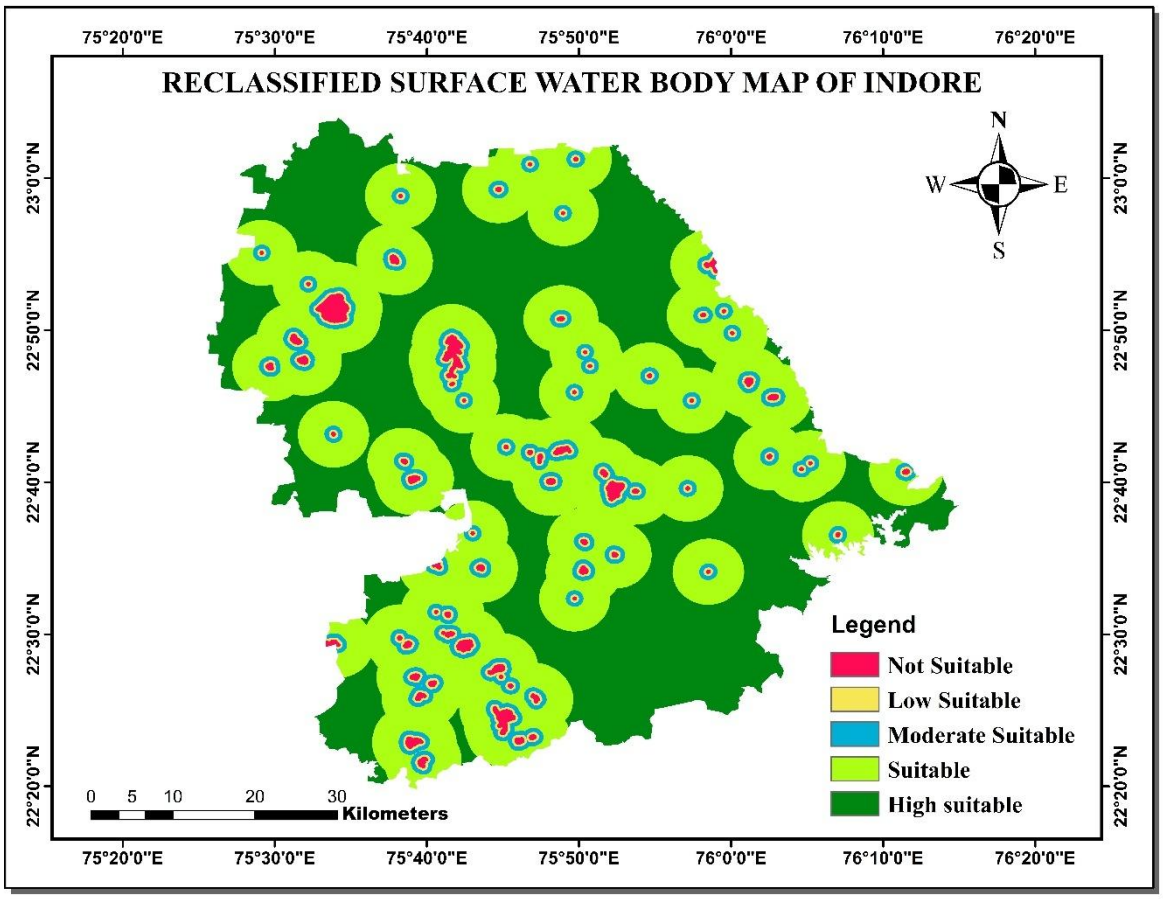

Figure 25: Reclassified surface water bodies map of Indore district

5.11.4 Proximity to Rivers/Streams

In addition to static water bodies, river and stream proximity were analysed separately due to their environmental sensitivity. A buffer of >4000 meters from rivers was assigned the highest suitability (score 5), while areas within 500 meters were considered unsuitable (score 1). The southern and western parts of the district had significant stretches of suitable land, while central zones near the Khan and Saraswati rivers were found to be unsuitable for industrial development.

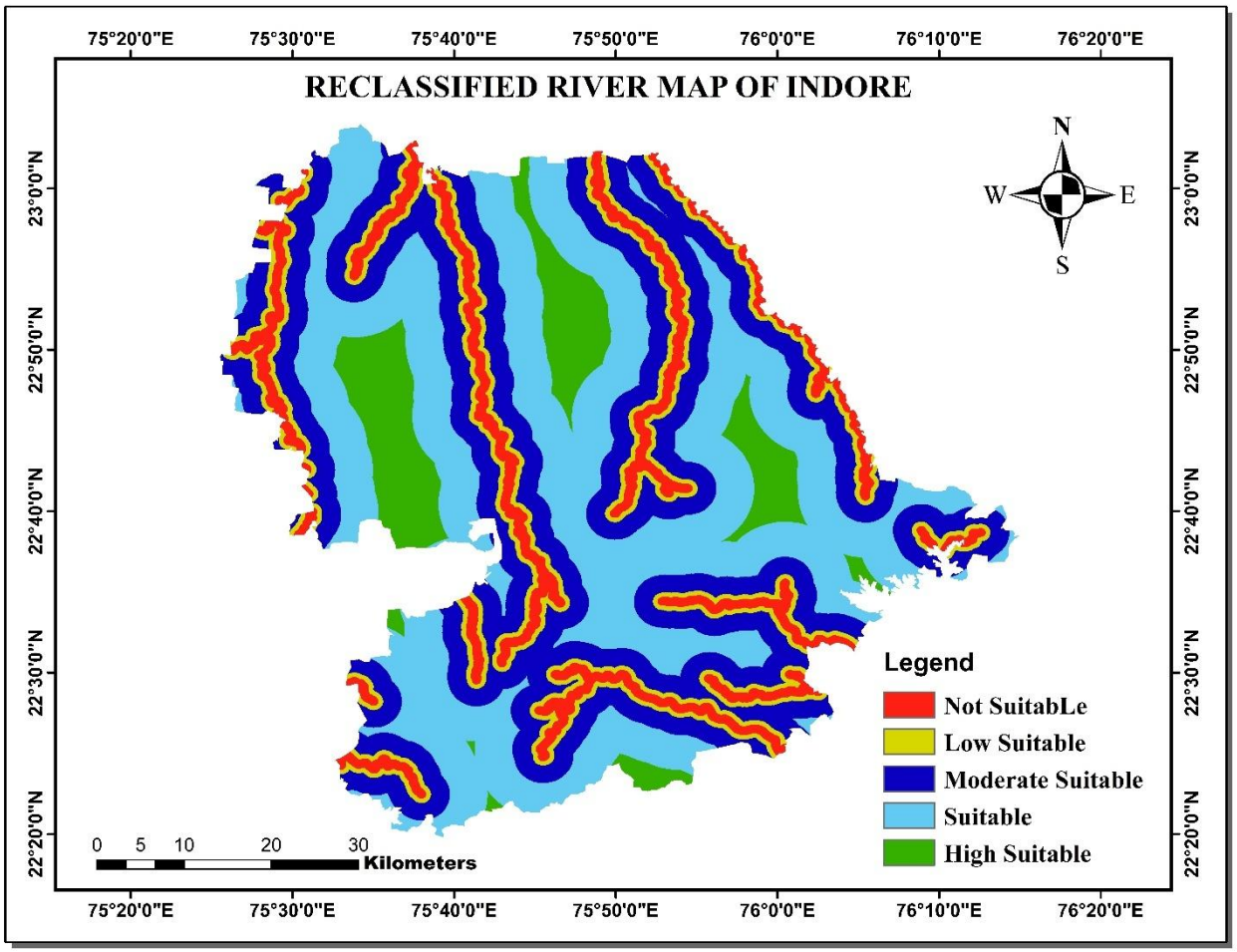

Figure 26: Reclassified River map of Indore district

5.11.5. Proximity to Industrial Areas

Proximity to existing industrial areas is a major factor for selecting a site, as it facilitates access to utilities and reduces the burden on new infrastructure. Areas within 1000 meters of industrial zones were ranked as highly suitable (score 5). The map analysis showed clusters of high suitability around Pithampur Industrial Area and regions south of the urban core, indicating favourable zones for plant establishment.

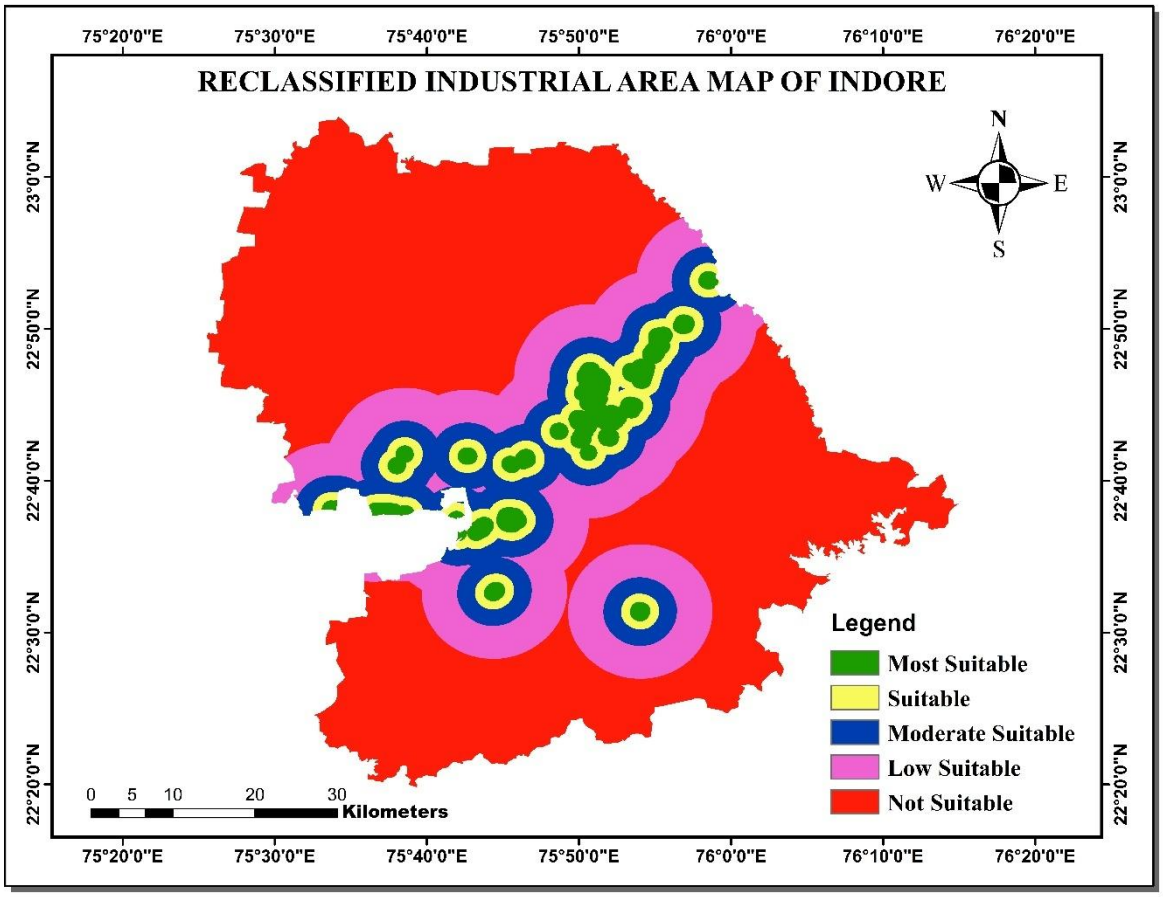

Figure 27: Reclassified industrial area map

5.11.6 Land Use and Land Cover (LULC)

LULC data is crucial in identifying locations with minimal environmental impact and legal restrictions. Areas categorised as barren or wasteland are more suitable for industrial development, while agricultural, forested, or residential zones are less favourable. In this study, LULC was derived from Esri Sentinel-2 satellite imagery, allowing for accurate classification of the land surface features within the Indore district.

.

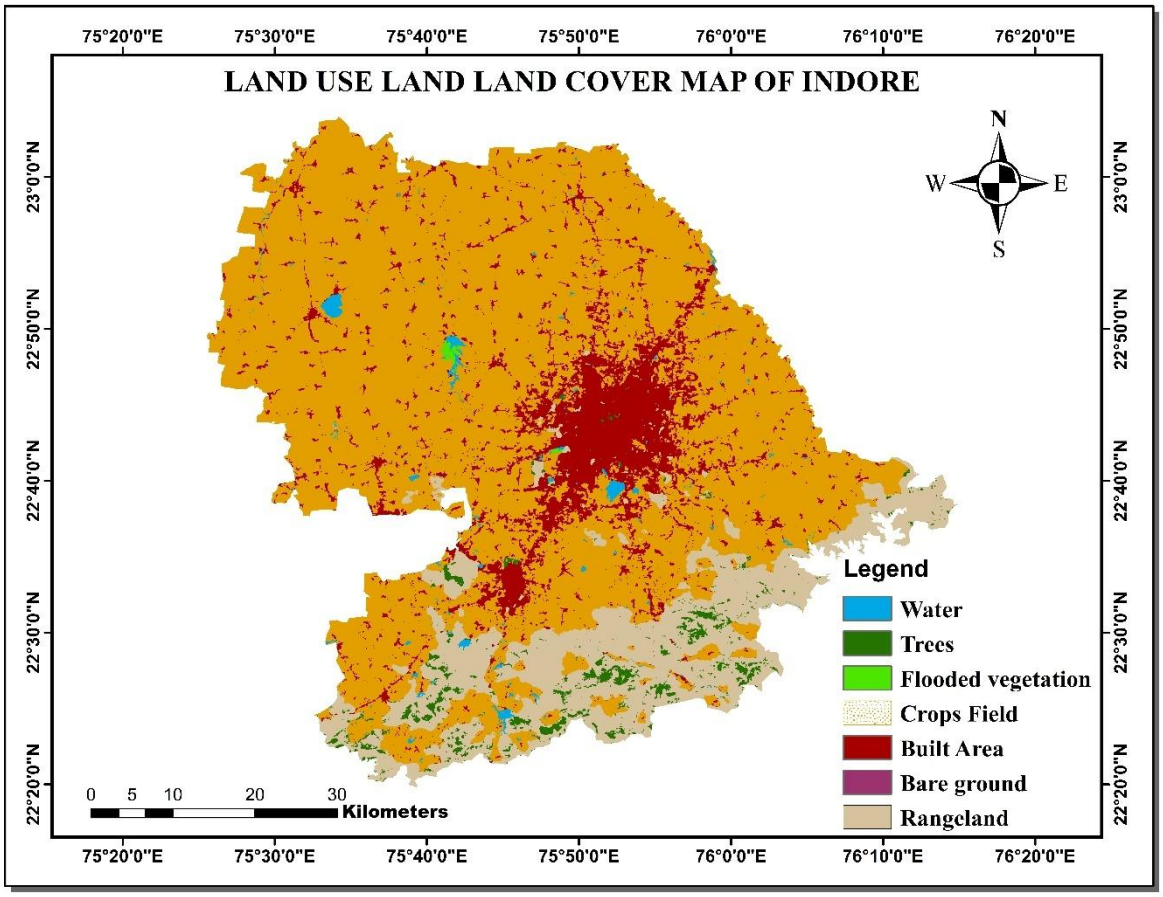

Figure 28: LULC 2024 map of Indore district

5.11.7 AHP multicriteria matrix and pair-wise comparison

The AHP approach can be used as a set of tools for deriving the weights of criteria. The AHP can deal with inconsistent judgments. The Pairwise Comparison Matrices involve comparing all the possible pairs of criteria in order to determine which of all the criteria is of a higher priority. To identify the potential sites for water conservation, site selection depends on the rating and the weights of each thematic layer.

Table 13: Pairwise comparison matrix

Column1	LULC	Industrial Area	Surface Water body	River	Road Network	Slope
LULC	1	1	4	5	6	8
Industrial Area	1	1	3	4	5	7
Surface Water body	0.25	0.33	1	2	4	5
River	0.2	0.25	0.5	1	3	5

Road Network	0.17	0.125	0.2	0.25	1	3
Slope	0.13	0.142	0.2	0.20	0.33	1
Sum	2.74	2.85	8.9	12.45	19.33	29

Table 14: Standardised matrix

STANDARDIZED MATRIX								
	LULC	**Industrial Area**	**Surface Water body**	**River**	**Road Network**	**Slope**	**AVG. Weight**	**Lambda**
LULC	0.3647	0.3507	0.4494	0.4016	0.3103	0.2759	0.36	6.4540
Industrial Area	0.3647	0.3507	0.3371	0.3213	0.2586	0.2414	0.31	6.3614
Surface Water body	0.0912	0.1169	0.1124	0.1606	0.2069	0.1724	0.14	6.2899
River	0.0729	0.0877	0.0562	0.0803	0.1552	0.1724	0.10	6.0680
Road Network	0.0608	0.0438	0.0225	0.0201	0.0517	0.1034	0.05	5.8921
Slope	0.0456	0.0501	0.0225	0.0161	0.0172	0.0345	0.03	6.0258
Sum	1	1	1	1	1	1	Max	6.4540

The final percentage weightage values of different layers are listed in a table prepared according to the AHP proposal, which reflects the number of criteria involved, as shown in Table 15

Table 15: AHP model percentage weightage

Sr No.	**Layer**	**Weightage (%)**
1	LULC	36
2	Industrial Area	31
3	Surface Water body	14
4	River	10
5	Road Network	5
6	Slope	3

5.12. LIB Recycling plant Suitability Analysis using Weighted Overlay

A weighted overlay analysis was conducted using ArcGIS software to identify suitable sites for a LIB recycling plant in Indore district, Madhya Pradesh. Six criteria layers were considered: Land Use and Land Cover (LULC), proximity to industrial areas, distance from surface water bodies, river/stream buffer zones, road network, and slope. Weights were assigned to each layer using the Analytical Hierarchy Process (AHP), with LULC (36%) and proximity to industrial areas (31%) contributing the most.

Each layer was reclassified into a common suitability scale (1–5), and integrated using the weighted overlay tool. The resulting suitability map (Figure 29) categorises the district into six classes: Restricted, Not Suitable, Low Suitable, Moderate Suitable, Suitable, and Most Suitable.

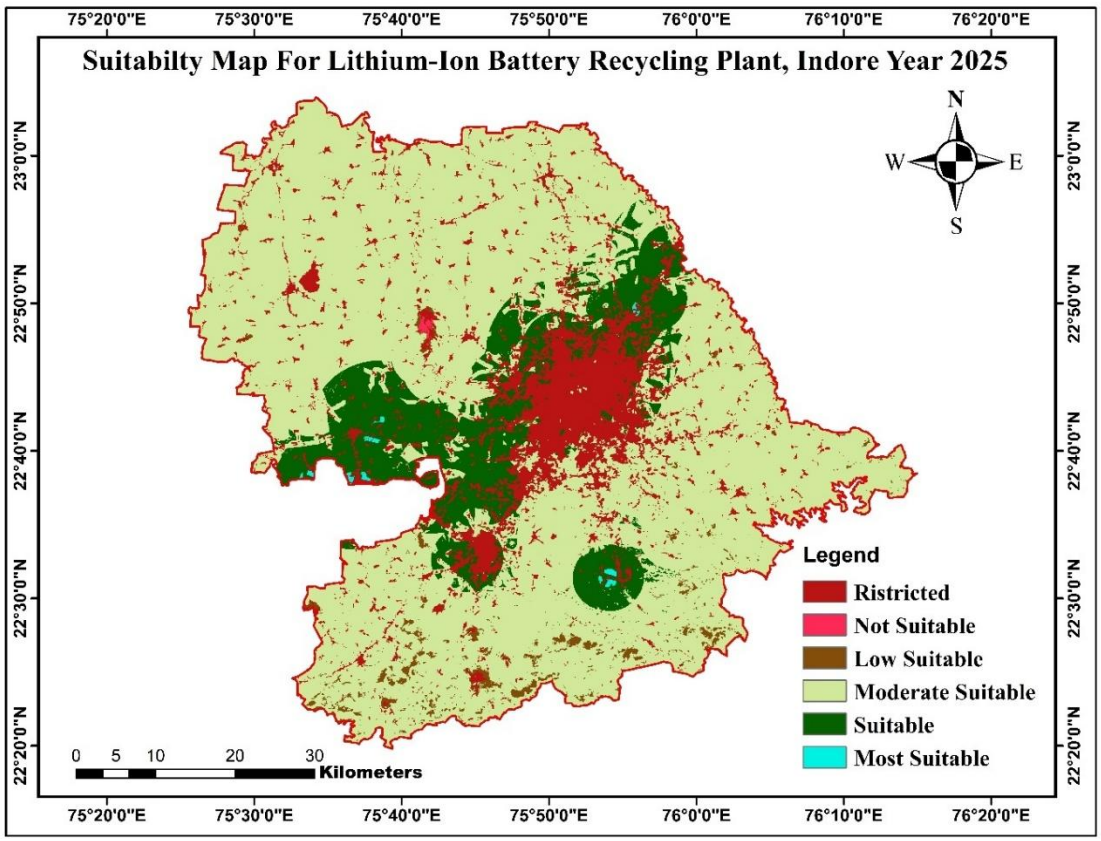

Figure 29: Land suitability map for EV recycling plant

The map reveals that areas with high to very high suitability are primarily concentrated in the western and southern parts of the district, particularly near Pithampur and existing industrial zones. These zones exhibit optimal land use, gentle slopes, sufficient distance from water bodies, and good road connectivity. In contrast, central and northeastern regions are dominated

by restricted or unsuitable areas due to high proximity to water bodies, dense urban settlements, or steep slopes. This spatial analysis provides a strategic decision-support framework for policymakers to identify environmentally and logistically appropriate sites for future recycling infrastructure.

Chapter 6

Conclusion

The transition to electric mobility in India, particularly in the two-wheeler segment, presents a promising pathway toward decarbonised transportation. However, this shift also introduces complex environmental and infrastructural challenges, particularly regarding the lifecycle management of lithium-ion batteries (LIBs). This study holistically addresses this issue by forecasting E2Ws sales, estimating future LIB waste, and identifying suitable locations for recycling infrastructure within the Indore district.

A Seasonal Autoregressive Integrated Moving Average (SARIMA) model, specifically SARIMA (3,2,3) (2,1,3) [12], was developed to forecast monthly E2Ws sales from November 2024 to December 2030. The model was validated through an 80-20 train-test split, achieving strong performance metrics: a **MAPE of 10.93%**, **RMSE of 13,897.8**, and **R^2 of 0.678**. Diagnostic checks confirmed the adequacy of the model, with residuals exhibiting white noise characteristics and no significant autocorrelation. Forecast results indicate a consistent upward trend in E2Ws adoption, with monthly sales expected to grow from approximately 120,000 units in late 2024 to over 340,000 units by the end of 2030.

Using these forecasts and industry-standard assumptions—specifically, a **specific energy of 210 Wh/kg** and an **average battery capacity of 2.025 kWh** per E2Ws—the study estimates a substantial rise in LIB waste generation. Annual battery waste is projected to grow from **17.17 million kg in 2025 to 37.02 million kg by 2030**, marking a more than twofold increase in just five years. Combined with historical data (2017–2024), the trend reveals three distinct phases: early adoption (minimal waste), rapid expansion (2021–2024), and sustained high-volume waste generation post-2025. This underscores the urgent need to develop EOL battery management frameworks and material recovery systems.

To tackle the spatial aspect of this new challenge, a site suitability assessment was done through multi-criteria GIS-based approaches to determine the best locations for the setting up of a battery recycling plant in Indore district, Madhya Pradesh. The study included the major influencing factors like proximity to urban areas, road and rail connectivity, population density, industrial areas, and environmentally sensitive areas. The outcomes identified a number of high-potential areas on the peripheries of Indore city, well located to serve both existing and

future flows of waste efficiently. The sites provide logistical benefits and environmental and land-use compliance opportunities for sustainable infrastructure development.

Through the combination of temporal prediction and spatial suitability analysis, this study provides an integrated framework for predicting and planning for the environmental impact of India's EVs revolution. This enables proactive policy development, industrial investment planning, and local implementation of battery recycling infrastructure. The results offer timely advice to national and regional stakeholders such as policymakers, urban planners, battery manufacturers, and waste management agencies.

Finally, this research adds significantly to the growing literature on circular economy strategies in electric mobility. By projecting future waste for batteries and determining where infrastructure must be established, it fills the data-driven planning-sustainable action gap, buttressing the significance of forward-looking strategies in the development of India's green transport future.

Future Scope

While this thesis offers a comprehensive approach to LIB waste forecasting and recycling site identification, several future research opportunities exist to expand and deepen the insights:

1. **Incorporating Other EV Segments:** Future studies could include electric three-wheelers, passenger vehicles, and public transport EVs to provide a more holistic estimation of national battery waste loads.
2. **Integration of Battery Second-Life Use:** Exploring second-life applications (e.g., stationary energy storage) before recycling would refine waste timelines and help optimise resource recovery strategies.
3. **Dynamic Lifespan and Degradation Models:** Integrating battery health data and real-world usage patterns could replace fixed-lifespan assumptions with more accurate, dynamic degradation curves.
4. **Policy Simulation and Demand Scenarios:** Incorporating various government incentive policies or technology diffusion scenarios could help forecast under different future adoption pathways.
5. **Real-time GIS Dashboard for Stakeholders:** A future extension could involve developing an interactive GIS-based decision-support tool for regulators and industries to visualise forecasted waste and infrastructure demand in real time.

REFERENCES

1) Ahmad, Z., Khan, M., & Ali, S. (2021). Economic and environmental benefits of lithium-ion battery recycling: A case study approach. IIUM Engineering Journal, 18(2), 238–252. https://doi.org/10.31436/iiumej.v18i2.773
2) Ai, N., Zheng, J., & Chen, W. Q. (2019). U.S. end-of-life electric vehicle batteries: Dynamic inventory modeling and spatial analysis for regional solutions. Resources, Conservation and Recycling, 145, 208–219. https://doi.org/10.1016/J.RESCONREC.2019.01.021
3) Akther, A., Ahamed, T., Noguchi, R., Genkawa, T., & Takigawa, T. (2019). Site suitability analysis of biogas digester plant for municipal waste using GIS and multi-criteria analysis. Asia-Pacific Journal of Regional Science, 3(1), 61–93. https://doi.org/10.1007/S41685-018-0084-2/FIGURES/12
4) Bandara, K., Hyndman, R. J., & Bergmeir, C. (2025). MSTL: a seasonal-trend decomposition algorithm for time series with multiple seasonal patterns. International Journal of Operational Research, 52(1), 79–98. https://doi.org/10.1504/IJOR.2025.143957;WGROUP:STRING:PUBLICATION
5) Box, G. (2013). Box and Jenkins: Time Series Analysis, Forecasting and Control. In A Very British Affair (pp. 161–215). Palgrave Macmillan UK. https://doi.org/10.1057/9781137291264_6
6) Box, G. E. P., Jenkins, G. M., & Reinsel, G. C. (2015). Time Series Analysis: Forecasting and Control (5th ed.). Wiley.
7) Box, G. E. P., Jenkins, G. M., Reinsel, G. C., & Ljung, G. M. (2016). JOURNAL OF TIME SERIES ANALYSIS BOOK REVIEW TIME SERIES ANALYSIS: FORECASTING AND CONTROL, 5TH EDITION, by. J. Time. Ser. Anal, 37, 709–711. https://www.wiley.com/en-us/Time+Series+Analysis%3A+Forecasting+and+Control%2C+5th+Edition-p-9781118675021
8) Boyden, A., Soo, V. K., & Doolan, M. (2016). The Environmental Impacts of Recycling Portable Lithium-Ion Batteries. Procedia CIRP, 48, 188–193. https://doi.org/10.1016/j.procir.2016.03.100
9) Chandio, I. A., Matori, A. N. B., WanYusof, K. B., Talpur, M. A. H., Balogun, A. L., & Lawal, D. U. (2013). GIS-based analytic hierarchy process as a multicriteria decision analysis instrument: A review. Arabian Journal of Geosciences, 6(8), 3059–3066. https://doi.org/10.1007/S12517-012-0568-8/FIGURES/4

10) Chen, H., Zhang, Y., & Wang, L. (2023). Circular economy perspectives on lithium-ion battery management: Opportunities and challenges ahead. Energies, 15(3), 1086–1100. https://doi.org/10.3390/en15031086
11) Dobó, Z., Dinh, T., & Kulcsár, T. (2023). A review on recycling of spent lithium-ion batteries. Energy Reports, 9, 6362–6395. https://doi.org/10.1016/J.EGYR.2023.05.264
12) Electric Vehicles: Electric Vehicle Industry in India and its Growth. (2021.-a). Retrieved May 22, 2025, from https://www.ibef.org/industry/electric-vehicle
13) Electric Vehicles: Electric Vehicle Industry in India and its Growth. (2021.-b). Retrieved May 29, 2025, from https://www.ibef.org/industry/electric-vehicle
14) Englberger, S., Hesse, H., Kucevic, D., & Jossen, A. (2019). A Techno-Economic Analysis of Vehicle-to-Building: Battery Degradation and Efficiency Analysis in the Context of Coordinated Electric Vehicle Charging. Energies 2019, Vol. 12, Page 955, 12(5), 955. https://doi.org/10.3390/EN12050955
15) Executive summary – Global EV Outlook 2022 – Analysis - IEA. (2022). Retrieved November 22, 2024, from https://www.iea.org/reports/global-ev-outlook-2022/executive-summary
16) Frith, J. T., Lacey, M. J., & Ulissi, U. (2023). A non-academic perspective on the future of lithium-based batteries. Nature Communications 2023 14:1, 14(1), 1–17. https://doi.org/10.1038/s41467-023-35933-2
17) Gaines, L. (2014). The future of automotive lithium-ion battery recycling: Charting a sustainable course. Sustainable Materials and Technologies, 1–2, 2–7. https://doi.org/10.1016/J.SUSMAT.2014.10.001
18) Gode, P., Bieker, G., & Bandivadekar, A. (2021). Battery capacity needed to power electric vehicles in India from 2020 to 2035. https://dhi.nic.in/writereaddata/fame/
19) Goyal, D. L. (2011). RS AND GIS BASED METHODOLOGY FOR THE PREPARATION OF A SUSTAINABLE DEVELOPMENT PLAN-A case study of Indore city.
20) How Weighted Overlay works—ArcGIS Pro | Documentation. Retrieved May 29, 2025, from https://pro.arcgis.com/en/pro-app/latest/tool-reference/spatial-analyst/how-weighted-overlay-works.htm
21) IEA. (2023). Trends in batteries – Global EV Outlook 2023 – Analysis - IEA. https://www.iea.org/reports/global-ev-outlook-2023/trends-in-batteries
22) Ifg. Decision Making Using the Analytic Hierarchy Process (AHP); A Step by Step Approach. Retrieved May 29, 2025, from http://www.iaras.org/iaras/journals/ijems
23) International Energy Agency (IEA). (2022). Global EV Outlook 2022. IEA.

24) Jaguemont, J., Boulon, L., Venet, P., Dube, Y., & Sari, A. (2016). Lithium-Ion Battery Aging Experiments at Subzero Temperatures and Model Development for Capacity Fade Estimation. IEEE Transactions on Vehicular Technology, 65(6), 4328–4343. https://doi.org/10.1109/TVT.2015.2473841

25) Johnson, R., Smith, T., & Lee, J. H. (2022). Global trends for waste lithium-ion battery recycling: A bibliometric analysis from 1984 to 2021. Minerals, 12(12), 1514–1528. https://doi.org/10.3390/min12121514

26) Kawadia, G., & Tiwari, E. (2017). Understanding Climate Change in Indore District: An Empirical Investigation of Trends and Shifts. Amity Journal of Economics AJECO Amity Journal of Economics, 2(1), 64–78.

27) Kaya, Ö., Alemdar, K. D., Atalay, A., Çodur, M. Y., & Tortum, A. (2022). Electric car sharing stations site selection from the perspective of sustainability: A GIS-based multi-criteria decision making approach. Sustainable Energy Technologies and Assessments, 52, 102026. https://doi.org/10.1016/J.SETA.2022.102026

28) Kim, S., Lee, P. Y., Lee, M., Kim, J., & Na, W. (2022). Improved State-of-health prediction based on auto-regressive integrated moving average with exogenous variables model in overcoming battery degradation-dependent internal parameter variation. Journal of Energy Storage, 46, 103888. https://doi.org/10.1016/J.EST.2021.103888

29) Kumar, J. A. V., Pathan, S. K., & Bhanderi, R. J. (2007). Spatio-temporal analysis for monitoring urban growth - a case study of Indore City. Journal of the Indian Society of Remote Sensing, 35(1), 11–20. https://doi.org/10.1007/BF02991829/METRICS

30) Kuo, C., Lin, Y., & Chen, C. Y. (2022). Life cycle assessment of lithium-ion batteries: Environmental impacts and mitigation strategies through recycling processes. Journal of Cleaner Production, 350, 131–145.

31) Lai, X., Chen, Q., Tang, X., Zhou, Y., Gao, F., Guo, Y., Bhagat, R., & Zheng, Y. (2022). Critical review of life cycle assessment of lithium-ion batteries for electric vehicles: A lifespan perspective. ETransportation, 12, 100169. https://doi.org/10.1016/J.ETRAN.2022.100169

32) Lee, K., Park, S., & Lee, J. S. H. (2022). Regulatory frameworks for lithium-ion battery disposal: Current status and future directions in sustainable practices. Environmental Science & Policy, 127, 15–24.

33) Liao, J., Longchamps, R. S., McCarthy, B. D., Shi, F., & Wang, C. Y. (2024). Lithium Iron Phosphate Superbattery for Mass-Market Electric Vehicles. ACS Energy Letters, 9(3), 771–778.

https://doi.org/10.1021/ACSENERGYLETT.3C02823/ASSET/IMAGES/LARGE/NZ3C02823_0005.JPEG

34) Liu, G., Wang, H., & Zhang, Q. Y. (2022). Recycling technologies for lithium-ion batteries: A review on hydrometallurgical approaches and their efficiencies in metal recovery processes. Journal of Hazardous Materials, 426, 130713.

35) Maisel, F., Neef, C., Marscheider-Weidemann, F., & Nissen, N. F. (2023). A forecast on future raw material demand and recycling potential of lithium-ion batteries in electric vehicles. Resources, Conservation and Recycling, 192, 106920. https://doi.org/10.1016/J.RESCONREC.2023.106920

36) Manuca, R., & Savit, R. (1996). Stationarity and nonstationarity in time series analysis. Physica D: Nonlinear Phenomena, 99(2–3), 134–161. https://doi.org/10.1016/S0167-2789(96)00139-X

37) Montaño Moreno, J., Palmer Pol, A., Sesé Abad, A., & Cajal Blasco, B. (2013). Using the R-MAPE index as a resistant measure of forecast accuracy. Psicothema, 4(25), 500–506. https://doi.org/10.7334/psicothema2013.23

38) Mrozik, W., Rajaeifar, M. A., Heidrich, O., & Christensen, P. (2021). Environmental impacts, pollution sources and pathways of spent lithium-ion batteries. Energy & Environmental Science, 14(12), 6099–6121. https://doi.org/10.1039/D1EE00691F

39) Navarro-Esbrí, J., Diamadopoulos, E., & Ginestar, D. (2002). Time series analysis and forecasting techniques for municipal solid waste management. Resources, Conservation and Recycling, 35(3), 201–214. https://doi.org/10.1016/S0921-3449(02)00002-2

40) Paparoditis, E., & Politis, D. N. (2018). The asymptotic size and power of the augmented Dickey–Fuller test for a unit root. Econometric Reviews, 37(9), 955–973. https://doi.org/10.1080/00927872.2016.1178887

41) Patel, R., Gupta, R., & Sharma, P. K. (2022). Environmental impacts of improper disposal of lithium-ion batteries: Risks and mitigation measures for sustainable waste management practices. Environmental Pollution, 292, 118–126.

42) Saaty, R. W. (1987). The analytic hierarchy process—what it is and how it is used. Mathematical Modelling, 9(3–5), 161–176. https://doi.org/10.1016/0270-0255(87)90473-8

43) Saaty, T. L. (2005). Analytic Hierarchy Process. Encyclopedia of Biostatistics. https://doi.org/10.1002/0470011815.B2A4A002

44) Saaty, T. L. (2014). Analytic Heirarchy Process. Wiley StatsRef: Statistics Reference Online. https://doi.org/10.1002/9781118445112.STAT05310

45) Schmuch, R., Wagner, R., Hörpel, G., Placke, T., & Winter, M. (2018). Performance and cost of materials for lithium-based rechargeable automotive batteries. Nature

Energy, 3(4), 267–278. https://doi.org/10.1038/S41560-018-0107-2;SUBJMETA=161,299,301,4077,4079,638,639,891;KWRD=BATTERIES,ELECTROCHEMISTRY,MATERIALS+FOR+ENERGY+AND+CATALYSIS

46) Smith, J., Brown, T., & Greenfield, L. A. (2023). Future trends in lithium-ion battery waste management: Leveraging advanced analytics for improved forecasting models. Resources Conservation & Recycling, 181, 106–115.

47) Tallman, K. R., Wheeler, G. P., Kern, C. J., Stavitski, E., Tong, X., Takeuchi, K. J., Marschilok, A. C., Bock, D. C., & Takeuchi, E. S. (2021). Nickel-rich Nickel Manganese Cobalt (NMC622) Cathode Lithiation Mechanism and Extended Cycling Effects Using Operando X-ray Absorption Spectroscopy. Journal of Physical Chemistry C, 125(1), 58–73. https://doi.org/10.1021/ACS.JPCC.0C08095/ASSET/IMAGES/LARGE/JP0C08095_0011.JPEG

48) Verma, M. A., & Bhonde, P. B. K. (2014). Optimisation of Municipal Solid Waste Management of Indore City using GIS. International Journal on Emerging Technologies, 5(1), 194–200.

49) Wang, X., Li, Y., & Zhang, X. F. (2021). Site suitability analysis for lithium-ion battery recycling plants using GIS: A case study approach. Sustainability, 13(4), 2100–2115.

50) Wen, Q., Gao, J., Song, X., Sun, L., Xu, H., & Zhu, S. (2019). RobustSTL: A Robust Seasonal-Trend Decomposition Algorithm for Long Time Series. Proceedings of the AAAI Conference on Artificial Intelligence, 33(01), 5409–5416. https://doi.org/10.1609/AAAI.V33I01.33015409

51) Xu, C., Li, J., & Lu, Y. (2021). Recycling and reuse of lithium-ion batteries: Current status and prospects. Renewable and Sustainable Energy Reviews, 135, 110202.

52) Yang, L., Yanhui, L., Yiyi, J., & Kiyoshi, F. (2024). Forecasting the echelon utilization potential of end-of-life electric vehicle batteries: a province-level investigation in China. Clean Technologies and Environmental Policy, 1–20. https://doi.org/10.1007/S10098-024-03072-X/TABLES/4

53) Zhang, J., Huang, H., Zhang, G., Dai, Z., Wen, Y., & Jiang, L. (2024). Cycle life studies of lithium-ion power batteries for electric vehicles: A review. Journal of Energy Storage, 93, 112231. https://doi.org/10.1016/J.EST.2024.112231

54) Zhang, X., Han, Y., & Zhang, W. (2021). A Review of Factors Affecting the Lifespan of Lithium-ion Battery and its Health Estimation Methods. Transactions on Electrical and Electronic Materials, 22(5), 567–574. https://doi.org/10.1007/S42341-021-00357-6/TABLES/1

55) Zhang, X., Li, W., & Meng, F. (2020). Estimation of lithium-ion battery waste in the future and its environmental impact. Journal of Cleaner Production, 276, 123976.
56) Zhang, Y., Li, Q., & Wang, Y. (2023). Innovations in lithium-ion battery recycling technologies: Enhancing recovery rates through advanced methodologies. Journal of Power Sources, 563, 231–240.
57) Zhang, Z., Jeong, Y., Jang, J., & Lee, C. G. (2022). A Pattern-Driven Stochastic Degradation Model for the Prediction of Remaining Useful Life of Rechargeable Batteries. IEEE Transactions on Industrial Informatics, 18(12), 8586–8594. https://doi.org/10.1109/TII.2022.3155597